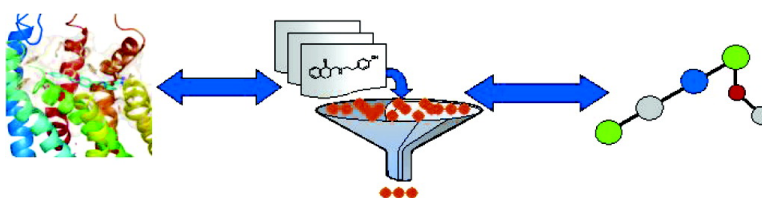


Virtual Screening of Biogenic Amine-Binding G-Protein Coupled Receptors: Comparative Evaluation of Protein- and Ligand-Based Virtual Screening Protocols

Andreas Evers, Gerhard Hessler, Hans Matter, and Thomas Klabunde

J. Med. Chem., **2005**, 48 (17), 5448-5465 • DOI: 10.1021/jm050090o • Publication Date (Web): 26 July 2005

Downloaded from <http://pubs.acs.org> on March 28, 2009



More About This Article

Additional resources and features associated with this article are available within the HTML version:

- Supporting Information
- Links to the 29 articles that cite this article, as of the time of this article download
- Access to high resolution figures
- Links to articles and content related to this article
- Copyright permission to reproduce figures and/or text from this article

[View the Full Text HTML](#)

Virtual Screening of Biogenic Amine-Binding G-Protein Coupled Receptors: Comparative Evaluation of Protein- and Ligand-Based Virtual Screening Protocols

Andreas Evers,* Gerhard Hessler, Hans Matter, and Thomas Klabunde

Aventis Pharma Deutschland GmbH, Ein Unternehmen der Sanofi-Aventis Gruppe, Chemical Sciences, Drug Design, 65926 Frankfurt am Main, Germany

Received January 31, 2005

In this paper, we compare protein- and ligand-based virtual screening techniques for identifying the ligands of four biogenic amine-binding G-protein coupled receptors (GPCRs). For the screening of the virtual compound libraries, we used (1) molecular docking into GPCR homology models, (2) ligand-based pharmacophore and Feature Tree models, (3) three-dimensional (3D)-similarity searches, and (4) statistical methods [partial least squares (PLS) and partial least squares discriminant analysis (PLS-DA) models] based on two-dimensional (2D) molecular descriptors. The comparison of the different methods in retrieving known antagonists from virtual libraries shows that in our study the ligand-based pharmacophore-, Feature Tree-, and 2D quantitative structure–activity relationship (QSAR)-based screening techniques provide enrichment factors that are higher than those provided by molecular docking into the GPCR homology models. Nevertheless, the hit rates achieved when docking with GOLD and ranking the ligands with GoldScore (up to 60% among the top-ranked 1% of the screened databases) are still satisfying. These results suggest that docking into GPCR homology models can be a useful approach for lead finding by virtual screening when either little or no information about the active ligands is available.

Introduction

In recent years, virtual screening has emerged as a complementary and alternative approach to high-throughput screening of large compound libraries.^{1,2} Usually, a virtual screening cascade is subdivided into different components that distinguish the level of complexity delivered as input. In the first step, target-unspecific filters are applied to eliminate chemical structures possessing non-druglike properties.³ Subsequently, topological searches⁴ from known ligands are often applied in virtual screening when seeking compounds with different structural characteristics.^{5–8} Because these methods do not require the calculation of three-dimensional (3D) conformers, they are suited for the rapid screening of huge databases. Given a bioactive (rigid) conformer of one or more ligands derived from structure determination methods or from molecular modeling, 3D-similarity⁹ or 3D-pharmacophore searches¹⁰ represent a further option for the virtual screening of compound libraries. Finally, when the 3D structure of the target protein is known or can be derived by homology modeling, the ligands that have passed previous filter steps can be subjected to molecular docking and scoring^{11–13} to provide potential candidates for experimental testing. There have been many recent publications describing the identification of novel ligands by receptor-based screening methods.¹⁴ The 3D target structures were derived by X-ray crystallography^{15–19} or homology modeling.^{20,21}

G-protein coupled receptors (GPCRs) represent one of the most important families of pharmaceutical tar-

gets.²² In particular, the subfamily of biogenic amine-binding GPCRs has provided excellent targets (given in brackets) for the treatment of several central nervous system (CNS) diseases, such as schizophrenia (mixed D2/D1/5-HT2), psychosis (mixed D2/5-HT2A), depression (5-HT1), or migraine (5-HT1). This GPCR subfamily has also provided drugable targets for other disease areas such as allergies (H1), asthma (beta2), ulcers (H2), or hypertension (alpha1 antagonist, beta1 antagonist). Because of the lack of crystal structures, computer-aided drug design for GPCRs has traditionally had to rely on either ligand-based modeling techniques^{23,24} or protein models, which are either generated de novo^{25–27} on the basis of the low-density map of bovine rhodopsin^{25–27} or generated by homology modeling based on the high-resolution crystal structure of bovine rhodopsin (e.g., refs 28–36). Because the sequence agreement between bovine rhodopsin and those GPCRs that are relevant for drug design is low and de novo modeling is considered not to be accurate enough,³⁷ there is an ongoing debate about whether these techniques provide GPCR models with an accuracy sufficient for drug design. Recent publications report successful applications of GPCR models in virtual screening (including molecular docking and scoring),^{28,38–40} indicating the general relevance of GPCR models and their usefulness for structure-based drug design. For example, Varady et al. performed a virtual screening for the D3 receptor using a homology model of this receptor. Out of 20 experimentally tested compounds, eight showed K_i values better than 1 μM .⁴⁰

In another attempt to explore the suitability of GPCR homology models for the purpose of virtual screening, we recently generated a homology model for the alpha1A receptor.³⁹ Applying two-dimensional (2D) queries and

* To whom correspondence should be addressed at Aventis Pharma Deutschland GmbH, Ein Unternehmen der Sanofi-Aventis Gruppe, Chemical Sciences, Drug Design, 65926 Frankfurt am Main, Germany. Phone +49(0)69305-12636. Fax +49(0)69331399. E-mail: Andreas.Evers@sanofi-aventis.com.

a 3D-pharmacophore model as a prefilter, we docked ~23 000 ligands into the alpha1A receptor homology model. Out of the 80 compounds that were selected for experimental testing, 37 showed a K_i value better than 10 μM , and 24 of these compounds were even binding in the submicromolar range. The hit rates achieved with these models were similar to those typically reached when the target protein is given by a crystal structure, suggesting that docking into rhodopsin-based GPCR models is indeed a feasible approach for the identification of novel ligands.

The general advantages of molecular docking are clear: assuming that near-native protein–ligand configurations are produced by the docking program, visual analysis of protein–ligand interactions allows for an intuitive interpretation and understanding of the binding process at the protein binding site. Furthermore, molecular docking might be able to identify novel ligands with a different binding mode, for example, by addressing novel interaction sites that have not yet been used by known ligands. It was indeed demonstrated that docking programs and scoring functions are well-suited for generating near-native ligand-binding poses in protein binding sites.⁴¹ However, the currently available scoring functions are still not considered applicable for accurate affinity prediction, even if the molecular protein–ligand interactions are available from crystal structures.^{42,43}

The sequential (filter) steps in a hierarchical screening approach are characterized by an increasing complexity with respect to their computational requirements. The increased effort of the more “expensive” methods can only be justified if these approaches provide higher enrichments and/or novel scaffolds of active compounds identified among the top-scored ligands. More and more recent publications report successful ligand identification by molecular docking into the X-ray structures or the homology models of target proteins.¹⁴ Sometimes, “high-throughput molecular docking” of entire virtual libraries is performed. However, the question of whether this method is more efficient than purely ligand-based approaches remains unanswered.

In this study, we compare different virtual screening strategies for identifying biogenic amine-binding GPCR antagonists from virtual libraries consisting of the antagonists of these target receptors (the alpha1A, 5HT2A, D2, and M1 receptors) and additional druglike molecules. For the screening of the virtual compound libraries, we use (1) molecular docking (using GOLD^{44–46} and FlexX-Pharm,^{47,48}) into GPCR homology models, (2) ligand-based pharmacophore models generated with Catalyst (Accelrys Inc.: San Diego, CA, 2002), or Feature Trees,^{6,49} (3) 3D-similarity searches using FlexS,⁹ and (4) statistical methods based on 2D molecular descriptors (CATS,^{50,51} MACCS,⁵² QikProp^{53,54}). The comparison of the different methods in retrieving known antagonists from the virtual libraries shows that the ligand-based screening techniques outperform the molecular docking approach when sufficient ligand information is used for the generation of models. In addition to the quantitative aspect of enrichment factors and hit rates, we will discuss representative examples to demonstrate the extent to which the generated models can

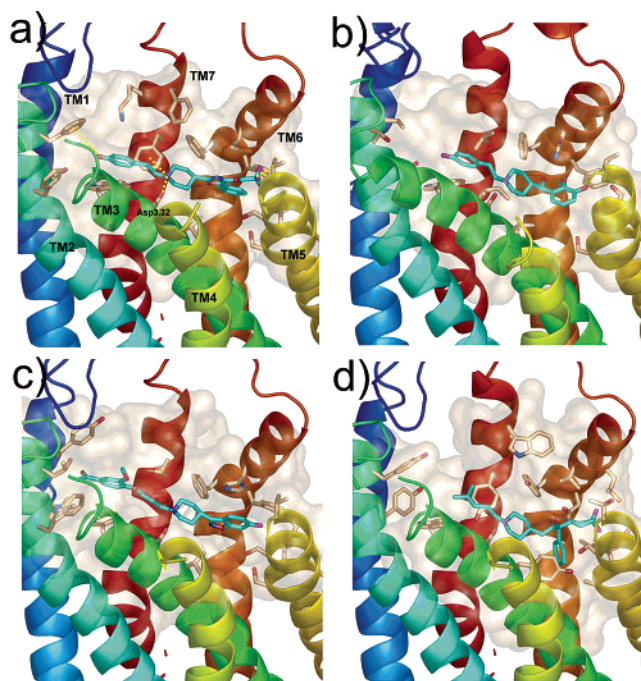


Figure 1. Homology models of four biogenic amine receptors complexed with ligands that were used for the construction and optimization of the protein models. (a) Homology model of the alpha1A receptor complexed with compound **1** from ref 70. (b) Homology model of the 5HT2A receptor complexed with MDL-100907.⁸⁶ (c) Homology model of the D2 receptor complexed with iloperidone.⁸⁷ (d) Homology model of the M1 receptor complexed with compound **12a** from ref 88.

serve to understand the determinants of molecular recognition and to provide guidance for compound optimization. These results show that the docking approach is most helpful for understanding how ligands of different chemotypes potentially bind to the receptors.

Methods

Screening Set: Training Sets for the Generation of 3D-Pharmacophore, Feature Tree, and 2D-Partial Least Squares (PLS) Models. For comparing the performances of the different virtual screening protocols, we compiled diverse screening data sets of 950 “inactive” compounds and 50 “active” compounds for each target, which were extracted from the MDL Data Drug Report (MDDR). The 3D-pharmacophore, Feature Tree, and 2D-PLS models were based on ligands extracted from the literature via Aureus. Details are described in the experimental section.

Model Generation and Retrospective Virtual Screening. Homology Models: Docking and Scoring. Protein models for the four target receptors were generated by applying ligand-supported homology modeling. The resulting models are shown in Figure 1. The ligands of the screening data sets were docked into the protein models using GOLD and FlexX-Pharm. In both cases, knowledge about ligand binding was included in the docking procedure in terms of interaction constraints. All docking poses were scored and ranked using different scoring functions (see Experimental Section).

Feature Tree and 3D-Pharmacophore Models. A multiple Feature Tree (MTree) model is conceptually similar to a 2D pharmacophore. It does not require the calculation of 3D coordinates and was shown to be very

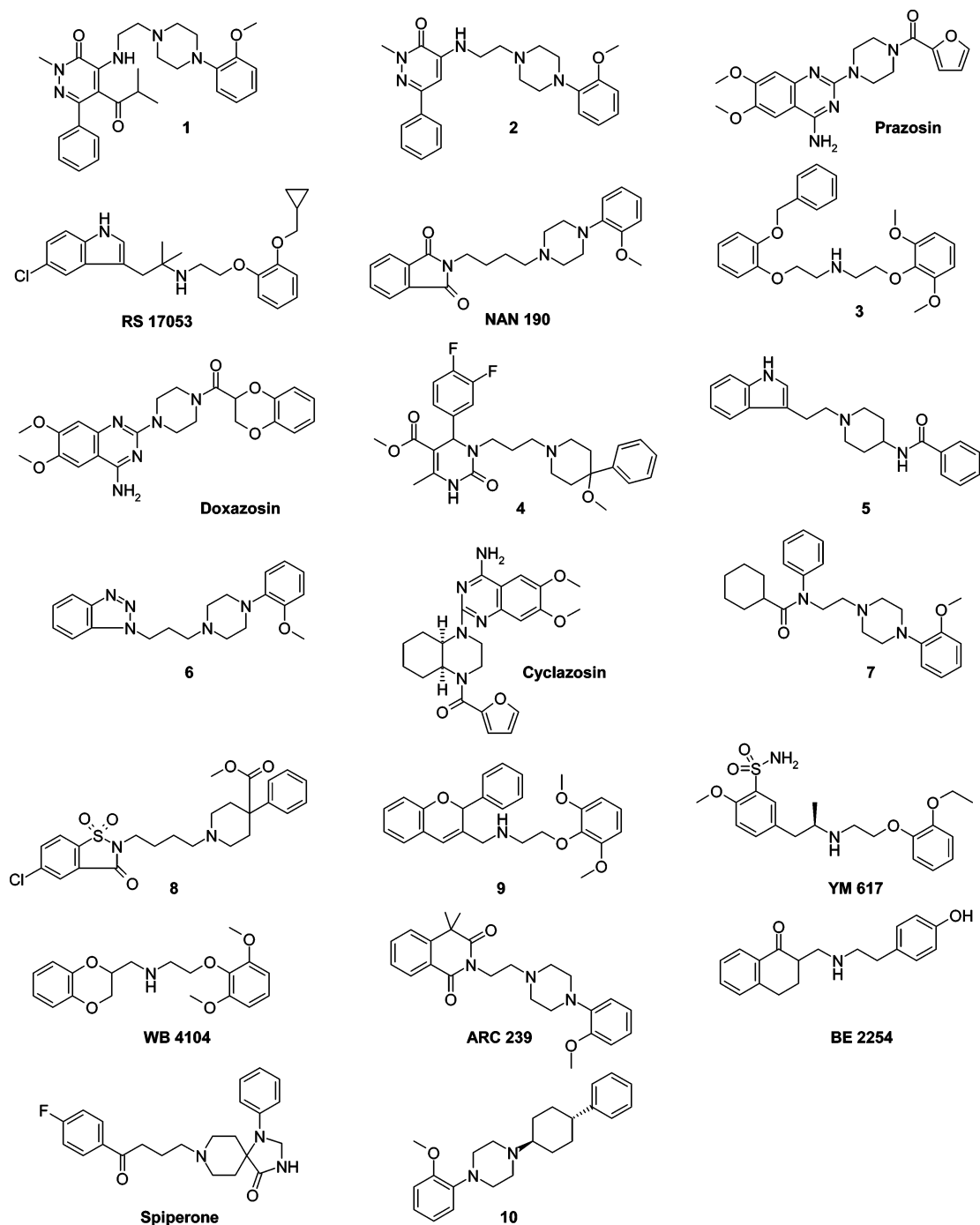


Figure 2. Alpha1A receptor antagonists used for the generation of the Catalyst pharmacophore and Feature Tree models. Structural analysis of the selected compounds revealed that they can be grouped into two classes. Class1 is represented by compounds 1–9, prazosin, NAN190, RS17053, doxazosin, and cyclazosin. Class2 is represented by YM617, WB4104, ARC239, BE2254, spiperone, and compound 10. The principal (representative) molecule for class1 is prazosin, and that for class2 is compound 10.

fast and efficient for the virtual screening of large databases. Catalyst was used for the generation of 3D-pharmacophore models and for the subsequent virtual screening of the screening data sets. To allow for a direct comparison of the performance of both methods for virtual screening, the same sets of ligands were used for the generation of MTree and 3D-pharmacophore models. For each target, two models were generated (“class1” and “class2”) on the basis of the ligands depicted in Figures 2–5.

Details of the model generation and the virtual screening are given in the experimental section and

depicted in Figure 6 (Feature Tree model). Figure 7 shows the 3D-pharmacophore models for the alpha1A receptor.

3D-Similarity Searching. 3D-similarity searches were performed for the four biogenic amine-binding GPCRs using the program FlexS for flexible superposition and similarity ranking of the screening sets. A critical issue when performing a 3D-similarity search is determining which compound to choose as a reference for the similarity search. We chose compound 1 (alpha1A), compound 12a (M1), MDL-100907 (5HT2A), and iloperidone (D2) (see Figure 1) for this purpose, that is,

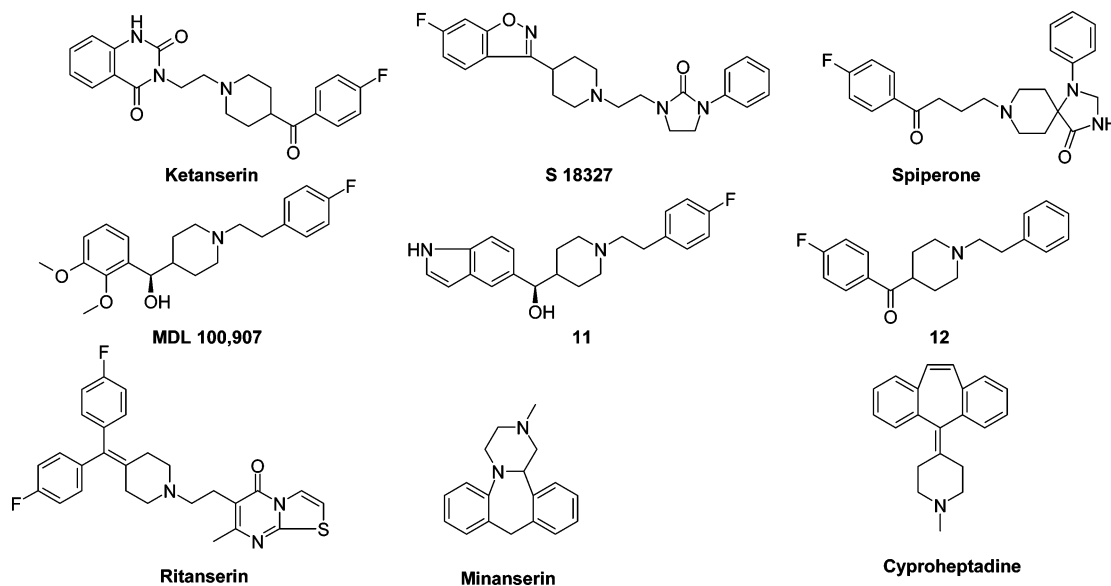


Figure 3. 5HT_{2A} receptor antagonists used for the generation of the Catalyst pharmacophore and Feature Tree models. Structural analysis of the selected compounds revealed that they can be grouped into two classes. Class1 is represented by ketanserin, S18327, spiperone, MDL-100907, and compounds 11 and 12. Class2 is represented by mianserin, ritanserin, and cyproheptadine. The principal (representative) molecule for class1 is spiperone, and that for class2 is mianserin.

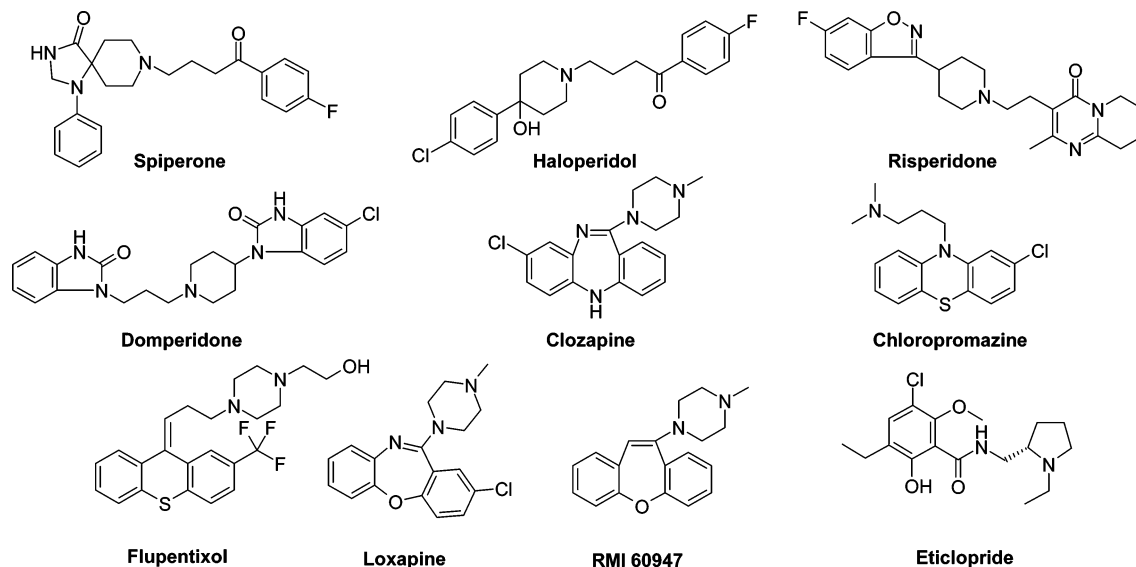


Figure 4. D₂ receptor antagonists used for the generation of the Catalyst pharmacophore and Feature Tree models. Structural analysis of the selected compounds revealed that they can be grouped into two classes. Class1 is represented by spiperone, haloperidol, risperidone, and domperidone. Class2 is represented by clozapine, chlorpromazine, flupentixol, RMI-60947, loxapine, and eticlopride. The principal (representative) molecule for class1 is spiperone, and that for class2 is clozapine.

for each target, only one compound was selected as the reference ligand.

2D-QSAR Models. A quantitative structure–activity relationship (QSAR) model relates the numerical properties of the molecular structure to its activity by a mathematical model. A wide range of 2D- and 3D-molecular descriptors has been used to describe the physicochemical and molecular properties of molecules (e.g., refs 51, 55–62). For the correlation of these descriptors with a biological activity, different techniques are available and have been extensively used for the development of QSAR models (e.g., refs 63–67). In the present study, we used 150 topological CATS descriptors,⁵¹ 163 MACCS keys,⁵² and 37 QikProp descriptors,^{53,54} for the physicochemical and molecular representation of chemical compounds. These were cor-

related with the affinities (pK_i values) of known ligands using PLS projection onto latent structures. Furthermore, we used sets of known active and inactive compounds for the generation of partial least squares discriminant analysis (PLS-DA) models. A detailed description of model generation is provided in the experimental section. Both models (PLS and PLS-DA) were used to rank the compounds of the screening data sets.

Results

In this section, the performance of the different methods in retrieving known antagonists of biogenic amine receptors from the respective screening sets will be evaluated. Furthermore, we will provide representative examples to demonstrate the extent to which these models can serve to understand the determinants of

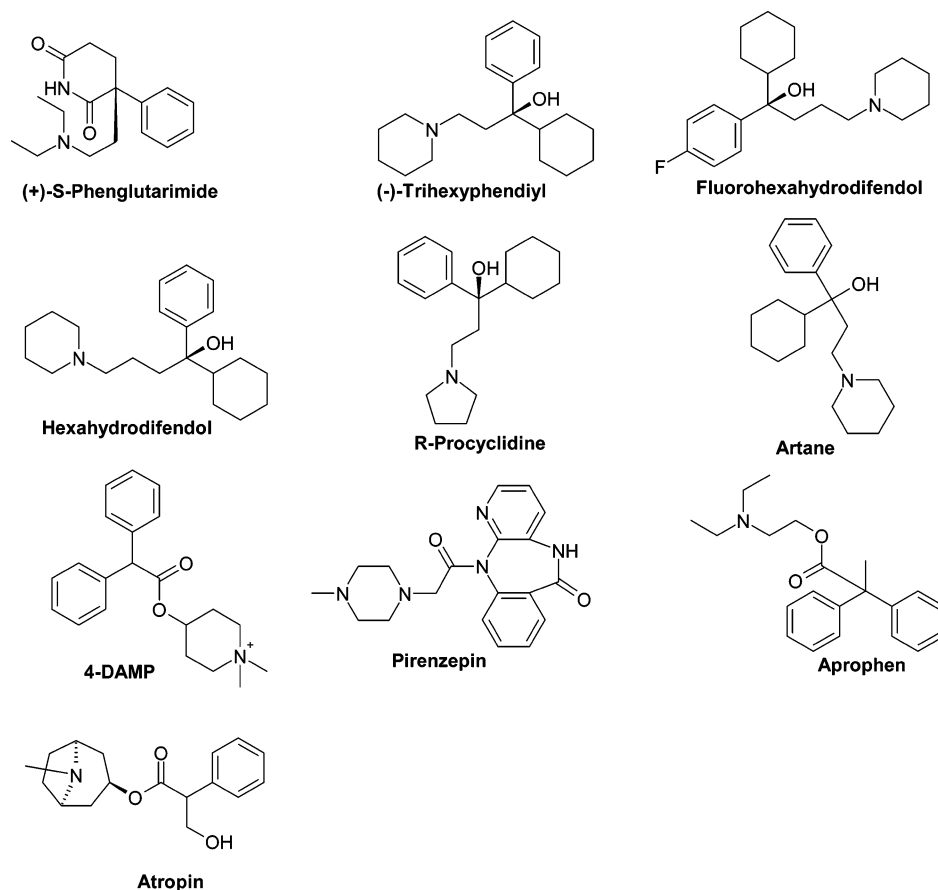


Figure 5. M1 receptor antagonists used for the generation of the Catalyst pharmacophore and Feature Tree models. Structural analysis of the selected compounds revealed that they can be grouped into two classes. Class1 is represented by phenglutarimide, trihexyphendiyl, fluorohexahydrodifendol, hexahydrodifendol, procyclidine, and artane. Class2 is represented by 4-DAMP, atropin, aprophen, and pirenzepin. The principal (representative) molecule for class1 is artane, and that for class2 is 4-DAMP.

molecular recognition at the investigated receptors and to provide guidance for compound optimization.

Homology Models: Docking and Scoring. Figure 1 depicts receptor–ligand complexes for the presented target GPCRs generated by ligand-supported homology modeling and validated by mutagenesis data.⁶⁸ In Figure 1a, proposed interactions for the alpha1A receptor, as derived from mutagenesis data and comparative affinity determinations based on ligand binding,^{69,70} are displayed as dashed lines. Analysis of this complex (Figure 1a) shows explicitly that Asp3.32 constitutes a central anchoring point for the ligands and divides the binding site into two different subpockets. The first subpocket, which is defined by helices 4, 5, 6, and 7, consists of amino acids offering hydrophobic side chains (Val5.39, Phe6.51, Phe6.52, Met6.55, Phe7.35, and Phe7.39). Similarly, the second subpocket is formed by mainly aromatic residues contributed by helices 1, 2, 3, and 7 (Phe2.60, Phe2.64, Trp3.28, Phe7.35, and Phe7.39). As an advantage, the docking procedure provides the user with easily interpreted binding modes of protein–ligand complexes. It helps one to understand features essential for molecular recognition based on the detailed analysis of interactions between the amino acids of the protein model and the docked ligands.

FlexX Docking. Enrichment curves resulting from the scoring of the docking poses generated by FlexX-Pharm are provided in Figure 8. A visual analysis of these curves reveals that the enrichments are lower than those obtained when screening with Feature Tree

or Catalyst models. An additional shortcoming is that there is no scoring function that provides acceptable enrichments for all four target receptors when considering the top-ranked compounds of the hit lists. G_SCORE provides the best enrichment for the 5HT2A receptor (enrichment factors of 0.0, 2.8, and 3.2 at the top-scored 1, 5, or 10% of the ranked database, respectively), XScore provides the best enrichments for the alpha1A (enrichment factors of 5.5, 3.5, and 2.6) and the M1 receptors (9.1, 4.3, 3.2), and PMF provides the best enrichments for the D2 receptor (0.0, 1.2, 1.4).

GOLD Docking. Figure 9 shows the enrichment curves resulting from scoring the docking poses generated by GOLD. Inspecting the first 10% of the ranked hit lists reveals better enrichments compared to those provided by FlexX-Pharm. Remarkably, in all cases, the best enrichments are obtained when GoldScore is used as scoring function. This observation simplifies a virtual screening protocol with GOLD. A rescoring of the generated ligand poses is not necessary because the GoldScore is returned as a final fitness value of GOLD's genetic search algorithm, which docks a ligand into the protein binding site. For the alpha1A receptor, enrichment factors of 12.0, 7.2, and 5.6 (at 1, 5, and 10% of the top-ranked data set, respectively) are observed (see also Table 1).

For the other receptors, the corresponding numbers are 12.0, 8.4, and 6.2 for the 5HT2A receptor, 4.0, 4.4, and 4.4 for the D2 receptor, and 12.0, 6.8, and 4.6 for the M1 receptor. These statistics are satisfactory. At this

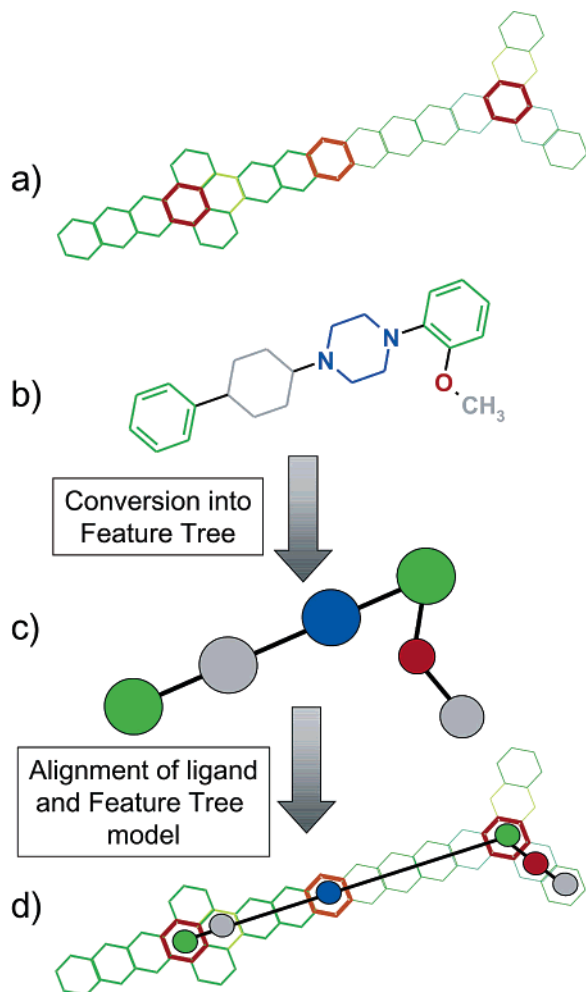


Figure 6. Generation of Feature Trees and mapping a ligand with a Feature Tree model. (a) The alpha1A Feature Tree model (class2) derived from six antagonists of the alpha1A receptor. The color code of individual hexagons in the model indicates the chemical similarity of aligned functional groups. Red hexagons indicate identical groups, orange and yellow hexagons indicate similar groups, and green hexagons indicate that there is no significant correspondence. (b) Alpha1A antagonist (compound **10**) with fragments colored according to their assigned physicochemical properties. Aliphatic fragments are gray, hydrogen-bond donors are blue, hydrogen-bond acceptors are red, and aromatic rings are green. (c) Feature Tree representation of compound **10** with molecular fragments converted into single nodes. Rings are merged into one node. Neighboring fragments (sharing atoms or bonds) are connected by edges. The Feature Tree and the molecule are shown in the same orientation. (d) Mapping of compound **10** onto the Feature Tree model (class2).

point it must be clearly noted that the docking poses of the ligands in the protein binding sites allow for an intuitive understanding of ligand binding, but the enrichments obtained by docking are lower than those resulting from the Feature Tree, Catalyst pharmacophore, and PLS-DA models (see the following sections).

As mentioned above, knowledge about ligand binding was included as an additional interaction constraint in the docking process. Indeed, a preliminary evaluation study with GOLD as the docking engine for the alpha1A receptor reveals lower enrichments compared to those including ligand information. If any information about ligand binding is ignored, then the enrichment factors

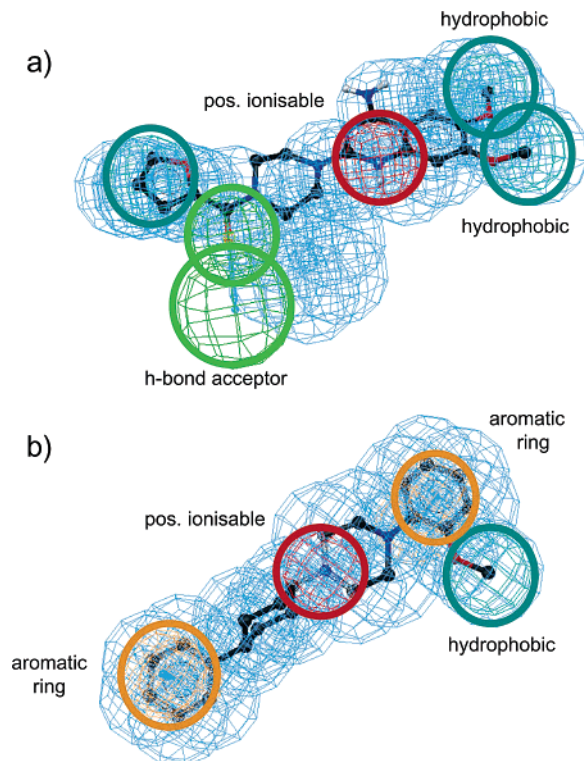


Figure 7. Catalyst pharmacophore models generated with Catalyst for the alpha1A receptor. Shown are the two pharmacophore models [class1 (a) and class2 (b)] mapping two different classes of high-affinity ligands (see Figure 2) of the alpha1A receptor.

for the alpha1A receptor are 7.3, 5.5, and 4.4 (at 1, 5, and 10% of the top-ranked data set, respectively).

3D-Pharmacophore and Feature Tree Models. Feature Tree Models. The enrichment curves for all MTree models are given in Figure 10, and the enrichment factors obtained at 1, 5, and 10% of the sampled databases are provided in Table 2.

In addition to the curves obtained from the individual MTree models, a consensus curve was derived for each target. This was accomplished by assigning each compound a *winner score*, that is, a higher similarity value assigned from the two individual (class1 and class2) queries. Analyzing the combined hit list (based on the winner score) for the 5HT2A receptor reveals an enrichment factor of 8.0 for active compounds (at 10% of the ranked database) compared to a random selection. In contrast, the enrichment factors obtained from the individual 5HT2A models only amount to 6.8 (model 5HT2A_class1) and 4.2 (model 5HT2A_class2). Similarly, the combination of the class1 and class2 models also results in higher enrichments for the alpha1A, M1, and the D2 receptors when the top 10% of ranked compounds is considered. When the portion of active compounds identified among the top-ranked 10% of the screened candidate database (“yield”) is considered, 80% (40 out of 50 compounds) of all 5HT2A antagonists are identified for the 5HT2A receptor. The corresponding yields of the individual 5HT2A models only amount to 68% (model 5HT2A_class1) and 42% (model 5HT2A_class2) of the active compounds among the top-ranked 10% hits. The performance of the combined hit lists of the MTree models is especially remarkable when only 10 of the top-ranked hits (corresponding to the top 1%) of the

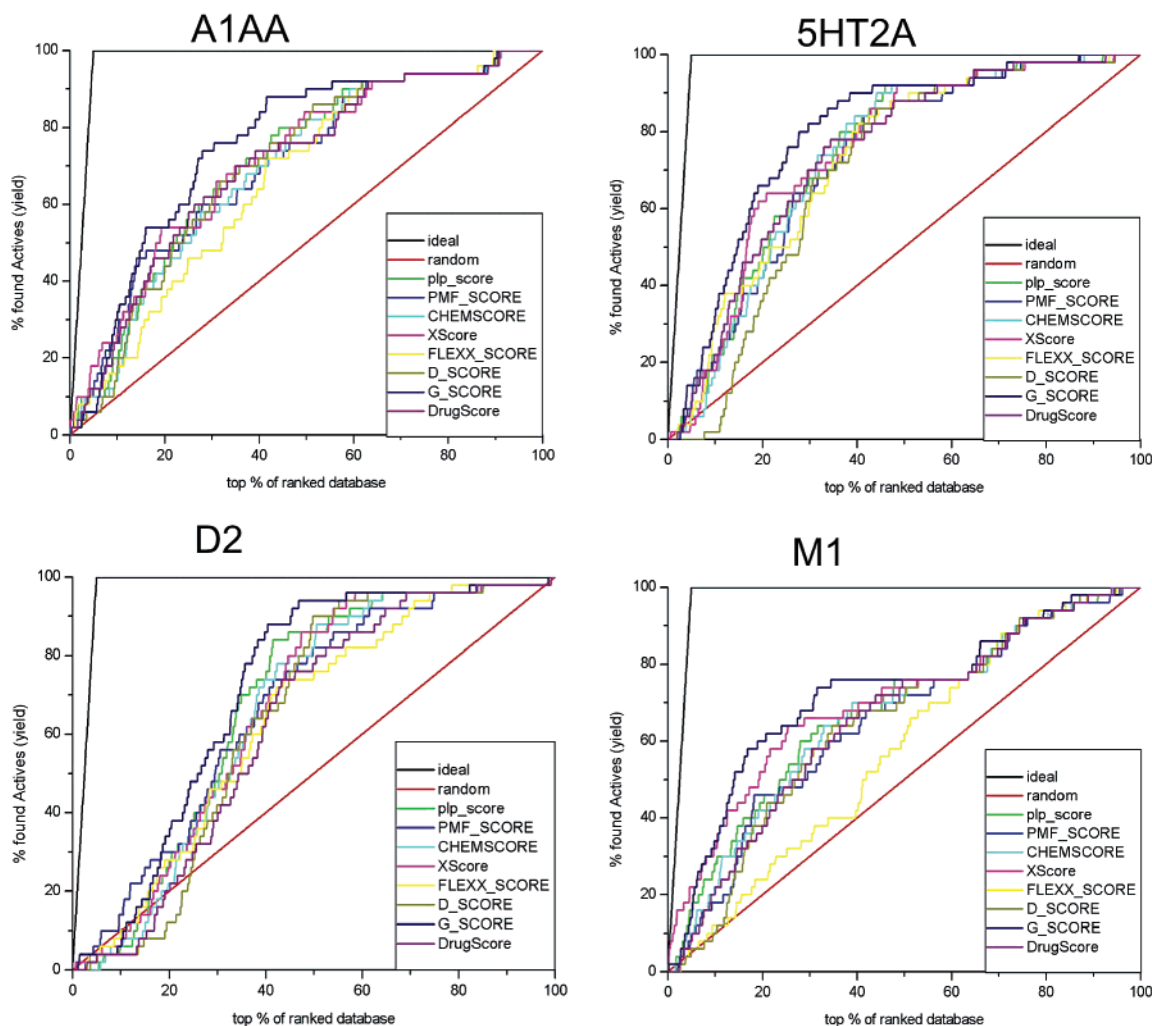


Figure 8. Enrichment curves obtained by docking into the alpha1A, 5HT2A, D2, and M1 receptor homology models with FlexX and scoring with eight different scoring functions.

screened database are considered. In the case of the 5HT2A, D2, and M1 receptors, all these compounds are antagonists of the respective receptors. Indeed, when only the top-ranked 1% of the screened databases is considered, the Feature Tree models outperform the other screening methods evaluated in this paper.

Figure 6a shows the Feature Tree model A1AA_class2, which is derived from six alpha1A antagonists (see Figure 2). The chemical similarities of aligned groups in the MTree model are indicated by the color codes of the hexagons, with the red hexagons representing identical groups, and the orange hexagons indicating highly similar nodes. As an example, the Feature Tree representation of compound **10** (Figure 6b) is given in Figure 6c. The alignment of this compound with model A1AA_class2 is provided in Figure 6d. The resulting 2D pharmacophore allows for an easy interpretation and is in good agreement with our knowledge about molecular recognition at the alpha1A receptor. As we already know from the analysis of the mutational data and the inspection of the alpha1A homology model, a central positively ionizable group (represented in Figure 6a by the orange hexagon) forms a charge-mediated hydrogen bond with Asp3.32, which is the key interaction for all biogenic amine-binding GPCRs.⁶⁸ Furthermore, in the alpha1A receptor, two hydrophobic subpockets are represented by the red-colored hydrophobic/aromatic

groups. These groups are connected to the central positively ionizable group by linkers of variable length.

3D-Pharmacophore Models. Figure 11 shows the enrichment curves obtained for both (class1 and class2) models of each target, and the enrichment factors at 1, 5, and 10% of the screened database are given in Table 2. Furthermore, the respective data for the combined hit lists (based on the winner scores) are provided.

Overall, the achieved enrichment and hit rates are slightly lower than those obtained by the Feature Tree models; however, the differences are not significant. In contrast to the Feature Tree models, a combination of the hit lists obtained from the individual (class1 and class2) models does not result in significantly better enrichments compared to the individual searches. Interestingly, the enrichment curves for the alpha1A receptor are steep in the beginning, going almost parallel to the ideal curve (black line). The flattening of the curves toward the right can be explained by the fact that some alpha1A antagonists cannot be mapped to the pharmacophore. In particular, the pharmacophore model A1AA_class1 based on the 14 class1 ligands (Figure 2) seems to be too restrictive to select all compounds in the test set.

In contrast to the Feature Tree models, the 3D-pharmacophore models require the calculation of the 3D-coordinates for each compound, resulting in an

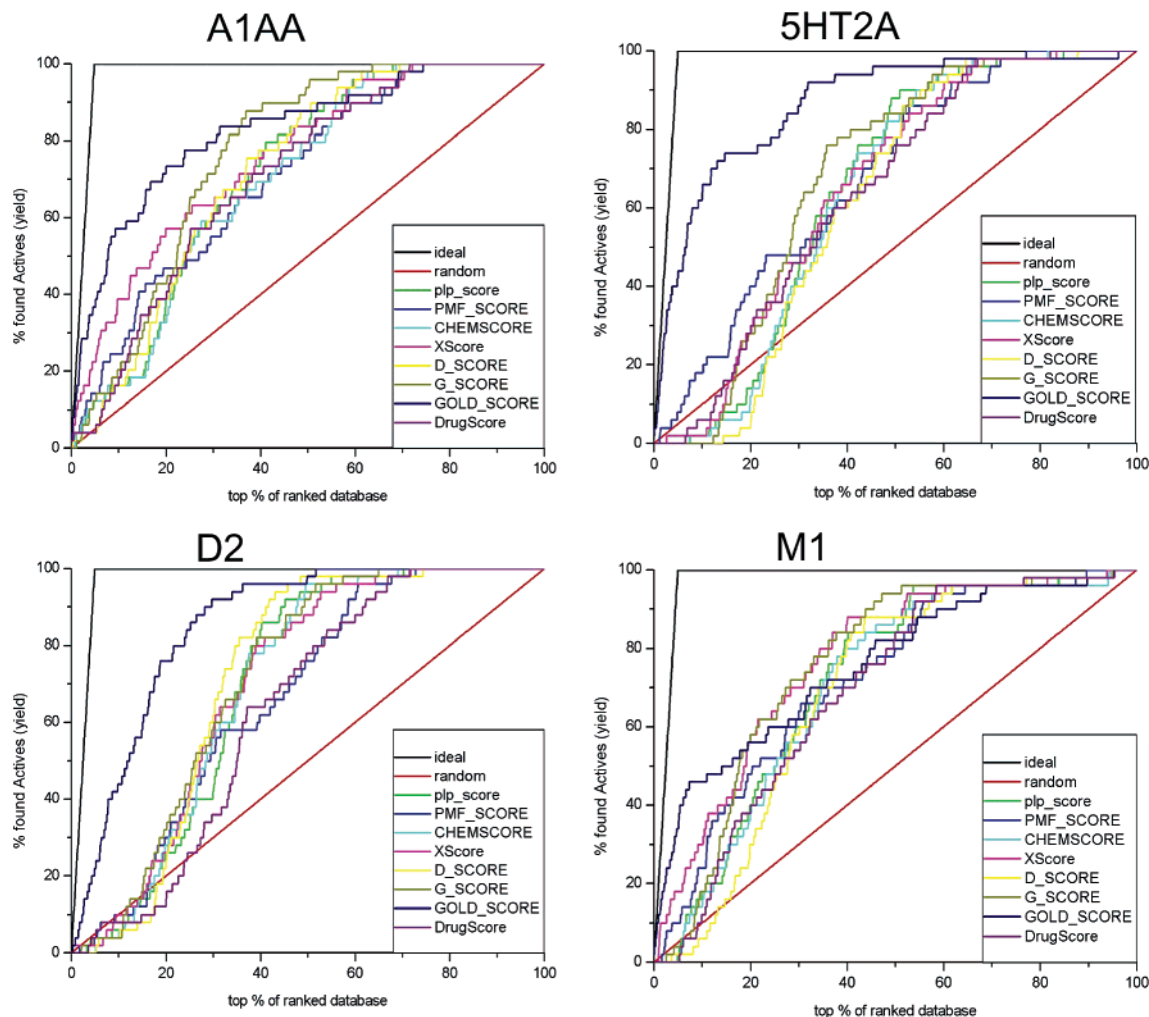


Figure 9. Enrichment curves obtained by docking into the alpha1A, 5HT2A, D2, and M1 receptor homology models with GOLD and scoring with eight different scoring functions.

Table 1. Enrichment Factors (EF) and Hit Rates of Active Compounds Obtained by Docking into the Corresponding Protein Models with GOLD and Scoring with GoldScore^a

% database screened	alpha1A		5HT2A		D2		M1	
	EF	hit rate [%]	EF	hit rate [%]	EF	hit rate [%]	EF	hit rate [%]
1	12.0	60	12.0	60	4.0	20	12.0	60
5	7.2	36	8.4	42	4.4	22	6.8	34
10	5.6	28	6.2	31	4.4	22	4.6	23

^a Enrichments and hit rates are given at 1, 5, and 10% of the ranked virtual libraries.

increased computational effort for model generation and database screening. Therefore, these models also allow for an intuitive interpretation of the 3D spatial arrangement of the features essential for binding at the target receptor. The alpha1A pharmacophore models are depicted in figures 7a (A1AA_class1) and 7b (A1AA_class2). Model A1AA_class2 contains a central positively ionizable pharmacophoric element, which probably interacts with Asp3.32. Comparative analysis of this pharmacophore model and the generated alpha1A homology model indicates that the two hydrophobic subpockets of the antagonist binding site are identified by the hydrophobic and aromatic pharmacophoric features. Some alpha1A antagonists contain an additional hy-

drogen-bond acceptor, which is reflected by pharmacophore model A1AA_class1.

The 3D-pharmacophore models of the alpha1A, 5HT2A, and D2 receptors have already been successfully used in another study to discriminate between the binders and the nonbinders of these receptors.⁷¹ In-house applications of the alpha1A 3D-pharmacophore models further revealed that these *in silico* tools can be used to guide the chemical optimization toward clinical candidates with fewer alpha1A-mediated side-effects (e.g., orthostatic hypotension, dizziness, and fainting spells).

3D-Similarity Searching. Table 3 provides the enrichment factors at 1, 5, and 10% of the screened database obtained from 3D-similarity searching with FlexS, and the enrichment curves are given in Figure 12.

Analyzing the enrichment factors (alpha1A: 1.8 at 1%, 0.8 at 5%, and 1.4 at 10% of the ranked database; 5HT2A: 3.6 at 1%, 2.4 at 5%, and 2.4 at 10% of the ranked database; D2: 1.8 at 1%, 2.0 at 5%, and 2.8 at 10% of the ranked database; M1: 1.8 at 1%, 0.4 at 5%, and 0.4 at 10% of the ranked database) shows results that are inferior to the results obtained from the other virtual screening techniques. The performance of these 3D-similarity searches could probably be improved by designating certain features as being essential (for

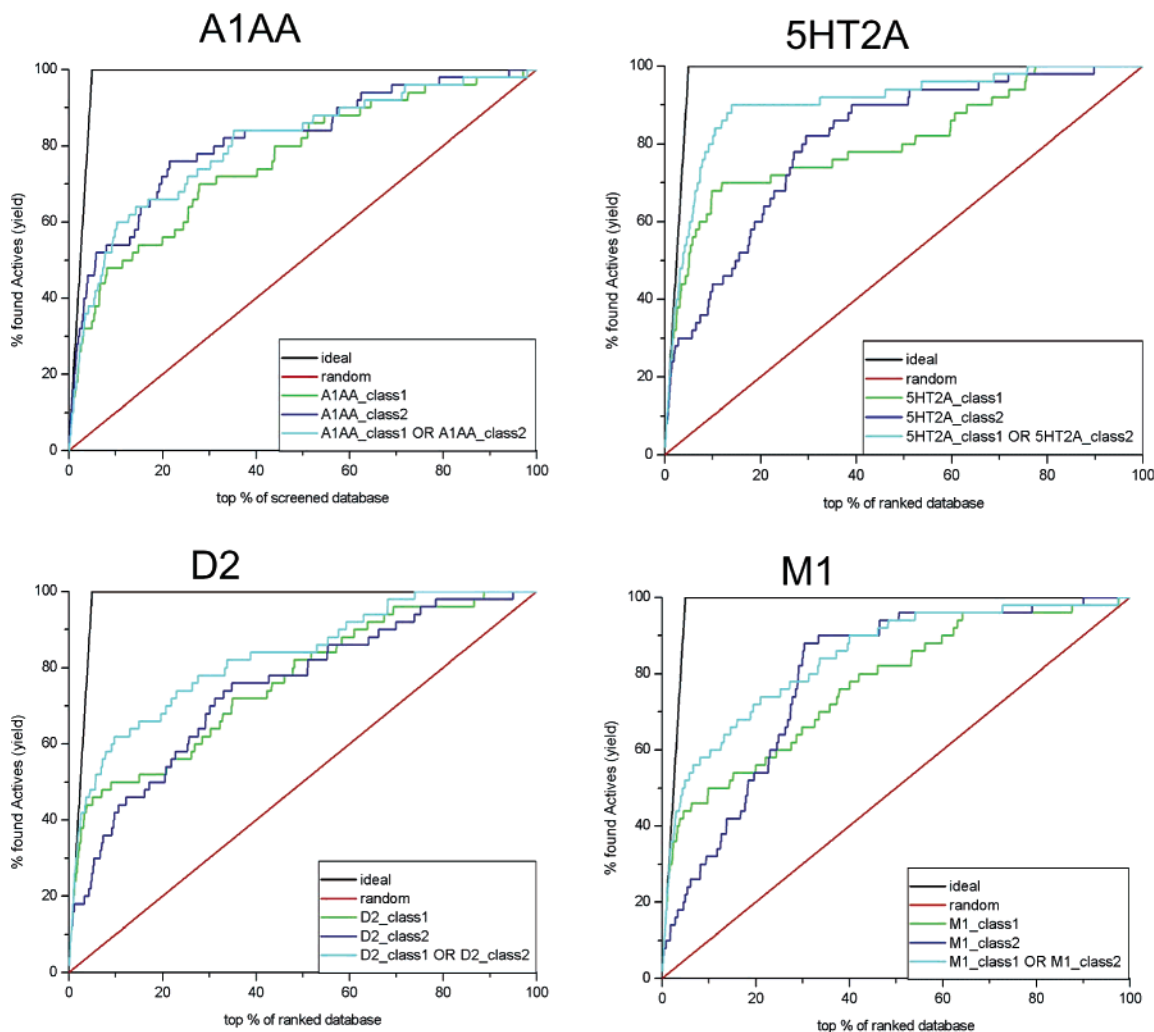


Figure 10. Enrichment curves obtained by Feature Tree models. For each receptor, three curves are shown. Class1 and class2 represent the enrichment curves obtained by screening with the corresponding (class1 or class2) models. Furthermore, a consensus curve (winner) was derived for each target. This was accomplished by assigning each compound a winner score, that is, a higher similarity value assigned from the two individual (class1 and class2) queries.

example, the matching of the positively ionizable nitrogen), which would conceptually be similar to a 3D pharmacophore. For example, comparing these 3D-similarity searches with the performance of the 3D-pharmacophore models is probably unfair because each pharmacophore model was generated on the basis of several (diverse) ligands, whereas the 3D-similarity searches were based only on one reference structure. One possibility for a “fair” comparison would be to merge several template ligands into one reference query. This can be done (within FlexS) by translating the molecular representations of several reference ligands into Gaussian representations and subsequently merging these Gaussians such that the molecular features that are similar in their 3D arrangement are more important than the features that are dissimilar. This procedure is again conceptually similar to a 3D-pharmacophore model.

2D-QSAR Models. Table 4 gives an overview of the statistics of the generated 2D-QSAR models. The hit rates and enrichment factors obtained from these models are provided in Table 5, and Figure 13 shows the corresponding enrichment curves.

PLS Models. For the alpha1A receptor, a six-component PLS model ($q^2 = 0.748$, $r^2 = 0.826$) was

obtained for 517 compounds. A six-component model was also derived for the M1 receptor ($q^2 = 0.675$, $r^2 = 0.771$) for 509 compounds. For the 5HT2A and D2 receptors, five-component models were obtained with $q^2 = 0.656$ and $r^2 = 0.740$ for the 5HT2A receptor (420 compounds) and $q^2 = 0.543$ and $r^2 = 0.685$ for the D2 receptor (544 compounds).

These models were subsequently employed to predict the affinities of the corresponding screening sets (see Figure 13 and Table 5). When one considers the PLS models, only the enrichment rates for the M1 receptor are acceptable. Here, the enrichment factors are 12.0, 5.6, and 4.0 at the top-scored 1, 5, or 10% of the ranked database. However, for the other targets, the respective enrichment factors are only 2.0, 1.2, and 1.2 for the alpha1A receptor, 0.0, 0.0, and 0.0 for the 5HT2A receptor, and 0.0, 0.0, and 0.2 for the D2 receptor.

The reasonable q^2 and r^2 values for all reported PLS models indicate their internal consistency. These models are able to accurately estimate the binding affinity for compounds of the respective training set. Because the training sets extracted from the Aureus database contain all ligands with reported K_i values (determined in a radioligand replacement assay) against the wildtype of the target receptors, it is likely that the prediction

Table 2. Enrichment Factors and Hit Rates from Screening the Virtual Screening Library Using the Alpha1A, 5HT2A, D2, and M1 Feature Tree and Catalyst Models^a

% database screened		alpha1A		5HT2A		D2		M1	
		EF	hit rate [%]	EF	hit rate [%]	EF	hit rate [%]	EF	hit rate [%]
Feature Tree models									
1	class1 ^b	12.0	60	18.0	90	20.0	100	18.0	90
	class2 ^c	16.0	80	16.0	80	16.0	80	10.0	50
	winner ^d	12.0	60	20.0	100	20.0	100	20.0	100
5	class1	6.8	34	9.6	48	8.8	44	8.8	44
	class2	9.2	46	6.0	30	5.2	26	4.4	22
	winner	7.6	38	11.2	56	9.6	48	10.4	52
10	class1	4.8	24	6.8	34	5.0	25	5.0	25
	class2	5.4	27	4.2	21	4.2	21	3.2	16
	winner	5.8	29	8.0	40	6.2	31	5.8	29
Catalyst models									
1	class1	14.0	70	10.0	50	6.0	30	18.0	90
	class2	12.0	60	8.0	40	2.0	10	16.0	80
	winner	14.0	70	10.0	50	0.0	0	16.0	80
5	class1	6.4	32	8.4	42	4.8	24	9.2	46
	class2	10.0	50	8.4	42	4.0	20	7.6	38
	winner	10.4	52	8.8	44	4.0	20	9.2	46
10	class1	3.6	18	4.4	22	2.8	14	5.6	28
	class2	5.4	27	6.4	32	4.4	22	5.0	25
	winner	5.8	29	7.4	37	4.6	23	5.6	28

^a Enrichments and hit rates are given at 1, 5, and 10% of the ranked virtual libraries. ^{b,c} For each receptor, two models were generated due to the observation that the ligand training sets can be grouped into two classes (class1 and class2) for each of the four targets. ^d A consensus score was derived for each target. This was accomplished by assigning each compound a winner score, that is, a higher similarity value assigned from the two individual (class1 and class2) queries.

accuracy is reasonable for the ligands of the active screening sets. However, information about inactive ligands is completely missing in the training data set. It was recently shown by Sheridan et al.⁷² that the prediction accuracy of QSAR models degrades as the molecules to be predicted depart from the training set. Indeed, the analysis of the predicted pK_i values indicates that the PLS model overestimates the affinities of the compounds from the inactive set, which do not have structurally similar compounds in the training sets of the PLS models. This inaccurate prediction for inactive compounds clearly indicates the inefficiency of the generated models with respect to virtual screening.

PLS-DA Models. As mentioned above, a PLS-DA model is generated for the prediction of the class membership (e.g., active or inactive) of an external set of objects. Statistics for the generated PLS-DA models are provided in Table 4. Models with reasonable significance were generated for each receptor, as indicated by the obtained q^2 and r^2 values. In contrast to the PLS models reported above, the performance of the PLS-DA models is superior in differentiating between binders and nonbinders for the respective GPCR screening sets (see Figure 13). For example, the enrichment factors obtained for the alpha1A receptor are 16.0, 11.2, and 7.6 at the top-scored 1, 5, or 10% of the ranked database (see Table 5). When the screening efficiencies of the different screening methods employed in this study are compared, the PLS-DA models perform best when the top-ranked 10% of the screened databases are considered. The PLS-DA models identify most of the active compounds for the alpha1A receptor (38 of 50 active compounds at 10% of the screened database), the 5HT2A receptor (40 of 50 active compounds), and the D2 receptor (36 of 50 active compounds). For the M1 receptor, 21 of 50 active compounds are identified at

10% of the screened database. Although this yield is lower than the hit rate achieved with the MTree models (which identified 29 of 50 active compounds), it is still acceptable.

This study suggests that the consideration of a chemically diverse set of inactive compounds in the training set to create classifiers instead of regression models based only on known active compounds is important for building virtual screening filters. Although the compounds of the decoy set are certainly not a complete representation of all inactive compounds at the target receptors, the achieved enrichments justify this pragmatic approach to extract a set of 1000 randomly chosen, inactive, structurally diverse compounds. As mentioned above, increasing the number of inactive compounds in the decoy set to 2000, 5000, or 10 000 compounds did not result in better enrichments for the active compounds.

At this point it should be noted that it is not the purpose of this paper to explore any optimal descriptor set and regression method for the generation of QSAR models suited for virtual screening. Comparable or even better results may be achieved using different sets of descriptors or QSAR methods. We chose the applied descriptors and PLS as the regression method because the loading plots resulting from a PLS analysis show the inner relationship between these descriptors and the biological activities, allowing for an unambiguous interpretation of the molecular features that are crucial for binding at the target receptor.

Figure 14 plots the product of the standard deviation of the considered 2D descriptors times the coefficient of the QSAR equation ($\text{COEFF} \times \text{STDEV}$) of the alpha1A PLS-DA model, indicating which descriptors are positively or negatively correlated with alpha1A activity. As indicated, the CATS descriptors DA_6 (i.e., the occurrence of a hydrogen-bond donor and a hydrogen-bond acceptor atom pair, separated by six bonds) and DL_6 (a hydrogen-bond donor and a lipophilic atom separated by six bonds) are positively correlated with activity at the alpha1A receptor. The mapping of this atom pair onto an alpha1A antagonist is given in Figure 14. The hydrogen-bond donors of both the DA_6 and the DL_6 descriptors are mapped onto the nitrogen, which is supposed to establish a hydrogen bond with Asp3.32. In addition, two MACCS keys, positively correlated with activity at the alpha1A receptor, can be mapped on this alpha1A antagonist (see Figure 14).

Discussion and Conclusion

In this contribution, we presented a comparative evaluation of different virtual screening approaches for identifying the known antagonists of four biogenic amine-binding GPCRs from a virtual library consisting of the antagonists of these receptors and additional druglike molecules. We compared the performance of different, well-established methods using molecular docking, 2D- and 3D-pharmacophore searches, 3D-similarity searches, and QSAR models based on topological 2D descriptors for the virtual screening of compound libraries. However, at this point it should be noted that the present study cannot provide an exhaustive comparison of all currently available virtual screening methods. Different and eventually better results

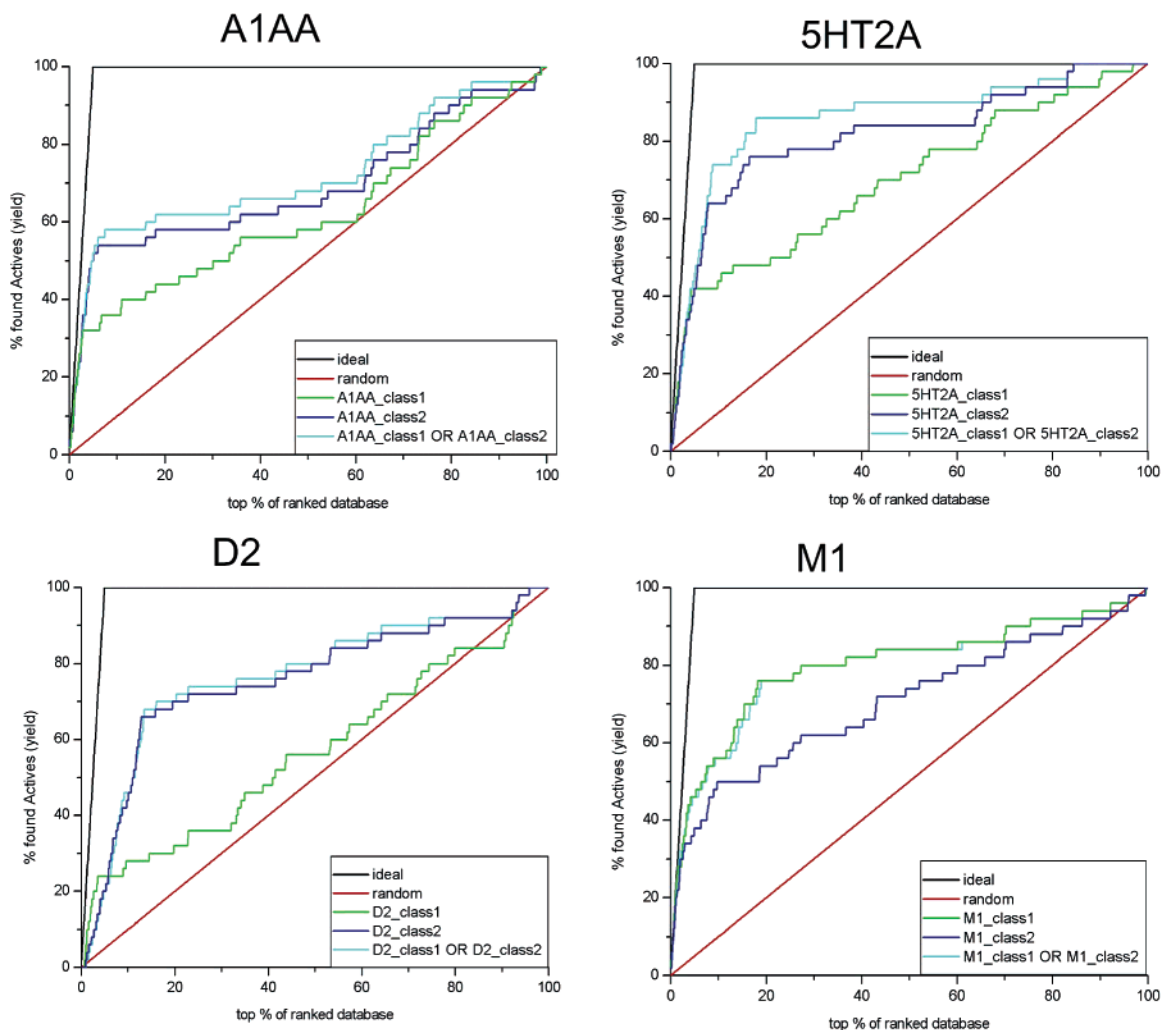


Figure 11. Enrichment curves obtained by Catalyst models. For each receptor, three curves are shown. Class1 and class2 represent the enrichment curves obtained by screening with the corresponding (class1 or class2) models. Furthermore, a consensus curve (winner) was derived for each target. This was accomplished by assigning each compound a winner score, that is, a higher fit value assigned from the two individual (class1 and class2) queries.

Table 3. Enrichment Factors and Hit Rates from Screening the Virtual Screening Library Using FlexS^a

% database screened	alpha1A		5HT2A		D2		M1	
	EF	hit rate [%]	EF	hit rate [%]	EF	hit rate [%]	EF	hit rate [%]
1	1.8	9	3.6	18	1.8	9	1.8	9
5	0.8	4	2.4	12	2.0	10	0.4	2
10	1.4	7	2.4	12	2.8	14	0.4	2

^a Enrichments and hit rates are given at 1, 5, and 10% of the ranked virtual libraries.

might have been obtained with other virtual screening approaches. For example, successful applications in virtual screening by molecular docking have been described in the literature using FRED (OpenEye Scientific Software), Glide (Schrödinger, Inc.), SLIDE,^{73,74} or DOCK.⁷⁵ 3D-pharmacophore searches can also be accomplished using tools such as UNITY (Tripos Inc., St. Louis, MO) or MOE (Chemical Computing Group, Montreal, Canada). Furthermore, as mentioned before, a wide range of 2D- and 3D-molecular descriptors are available for the development of models suited for virtual screening. The performance of the virtual screening methods used in this study was evaluated by assessing the hit rates and enrichments of known active

compounds within the top-scored compounds. In addition, graphical representations of the generated models were provided to demonstrate how these results increase the understanding of determinants for molecular recognition at their target receptors.

When the results are considered only with respect to hit rates and enrichment factors, the ligand-based approaches performed better than the protein-based approach (i.e., docking into the homology models). One might argue that for the protein-based virtual screening shown here, the protein structure is represented by a homology model rather than a crystal structure, and the lower resolution of the protein structure might be the cause for inaccurate docking poses and affinity estimations provided by the scoring functions. McGovern and Shoichet compared the performance of molecular docking against holo, apo, and modeled conformations of enzymes for 10 targets.⁷⁶ In their study, the best overall enrichment was produced by the holo (crystal) structure in seven systems, the apo (crystal) structure in two cases, and the modeled structure in one system. The authors suggested that the performance of the docking calculation is indeed affected by the particular representation of the receptor used in the screen and that

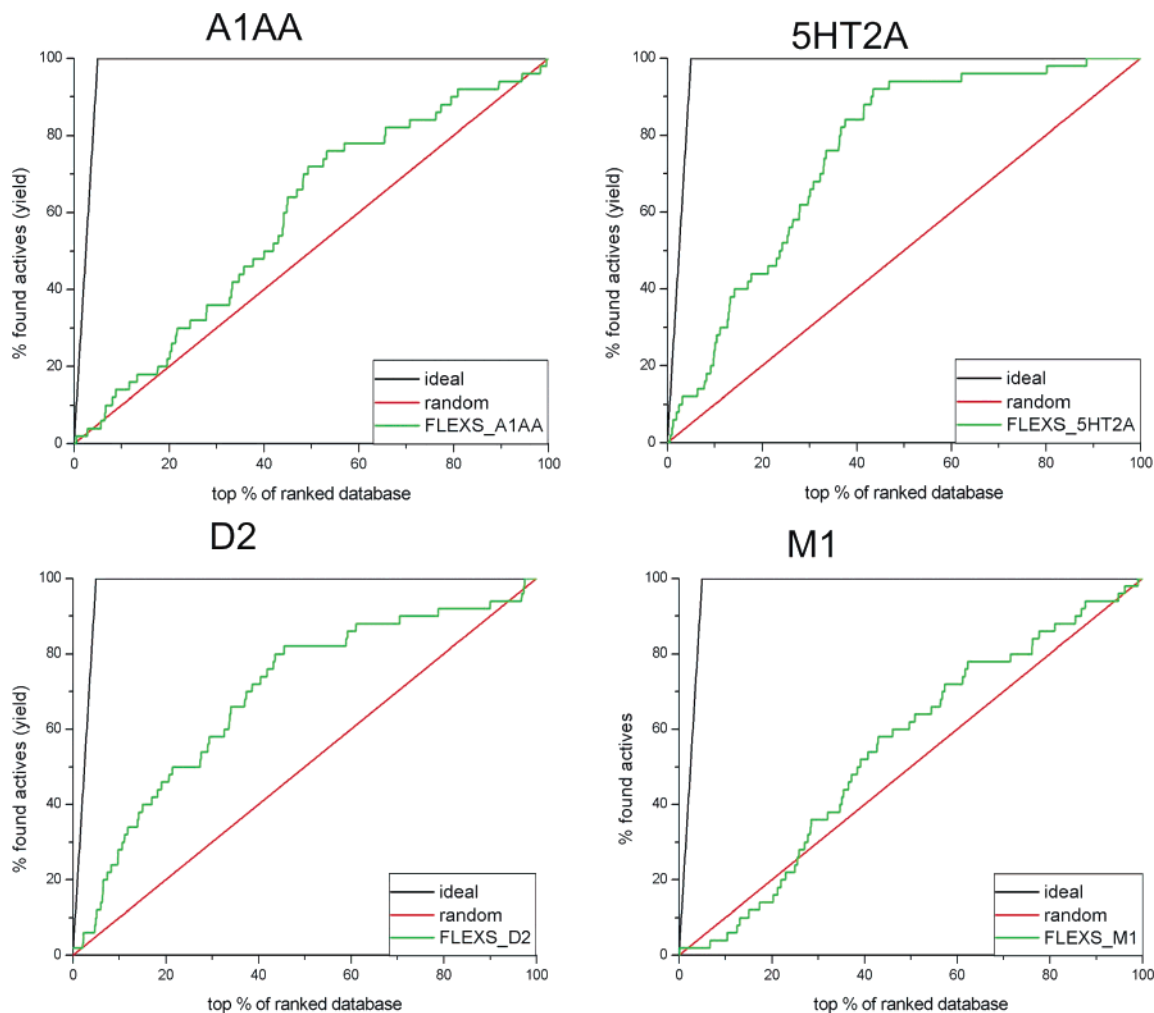


Figure 12. Enrichment curves obtained from 3D-similarity searching using FlexS.

Table 4. QSAR Statistics for the Training Data Sets of the PLS and PLS-DA Models

	no. of compounds	pK_i range	no. of components	q^2 (LOO)	r^2
2D-PLS model					
alpha1A	517	4.0–10.4	6	0.748	0.826
5HT2A	509	4.0–10.2	5	0.656	0.740
D2	420	3.8–9.2	5	0.543	0.685
M1	544	3.3–10.8	6	0.675	0.771
2D-PLS-DA model					
alpha1A	1468	0/1 ^a	6	0.910	0.925
5HT2A	1378	0/1 ^a	6	0.906	0.926
D2	1287	0/1 ^a	6	0.898	0.913
M1	1410	0/1 ^a	6	0.840	0.864

^a Instead of pK_i values, a class membership variable (Y) was assigned to each active ($Y = 1$) and inactive ($Y = 0$) compound for the generation of the PLS-DA model.

the holo (crystal) structure is the one most likely to yield the best discrimination between known ligands and decoy molecules, but important exceptions also emerged from their study. In an internal study (unpublished data), we recently docked 50 diverse cyclooxygenase-2 (COX-2) inhibitors and a test set of 950 inactive compounds (both extracted from the MDDR) into the high-resolution crystal structure of COX-2 (pdb-code: 6cox) and obtained enrichments similar to those obtained after docking into the GPCR homology models (9.0, 4.8, and 3.6 at the top-scored 1, 5, or 10% of the ranked database). This observation suggests that the

Table 5. Enrichment Factors and Hit Rates of Active Compounds Obtained by the PLS and PLS-DA Models^a

% database screened	alpha1A		5HT2A		D2		M1	
	EF	hit rate [%]	EF	hit rate [%]	EF	hit rate [%]	EF	hit rate [%]
2D-PLS model								
1	2.0	10	0.0	0	0.0	0	12.0	60
5	1.2	6	0.0	0	0.0	0	5.6	28
10	1.2	6	0.0	0	0.2	1	4.0	20
2D-PLS-DA model								
1	16.0	80	14.0	70	14.0	70	6.0	30
5	11.2	56	12.8	64	10.8	54	6.4	32
10	7.6	38	8.0	40	7.2	36	4.2	21

^a Enrichments and hit rates are given at 1, 5, and 10% of the ranked virtual libraries.

performance of a virtual screening based on molecular docking depends not only on the quality of the underlying protein structure but also on the employed docking program and scoring function. Indeed, recent evaluation studies performed by others have shown that the most limiting factor in ligand docking is probably that the currently available scoring functions are not yet generally applicable for accurate affinity prediction, even if the molecular protein–ligand interactions are available from crystal structures.^{42,43} Thus, it is difficult to determine how much the performance of virtual screening by molecular docking is affected by the “low resolu-

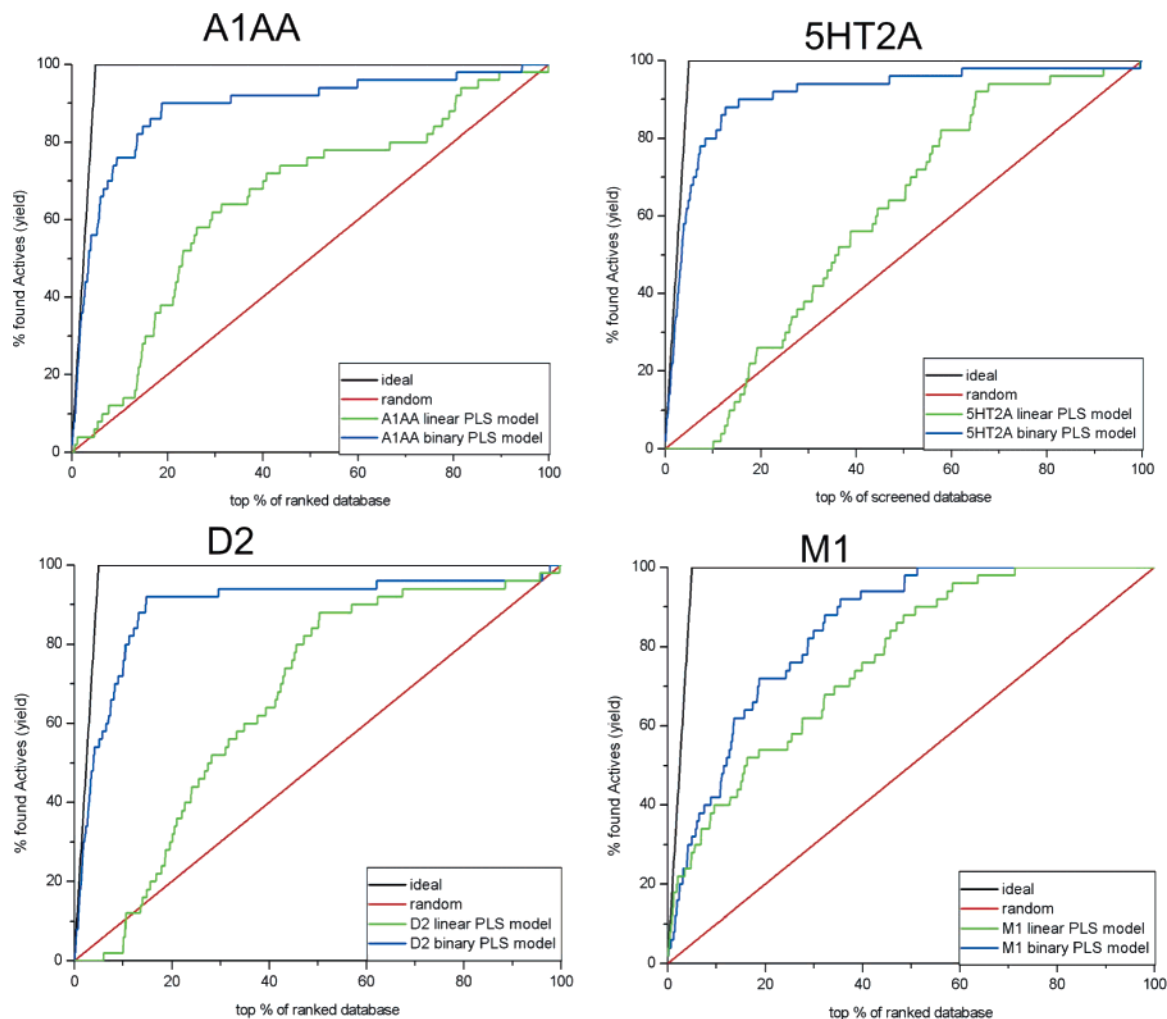


Figure 13. Enrichment curves obtained by PLS models. For each receptor, two curves are shown, representing the enrichment obtained by screening with either the PLS model or the PLS-DA model.

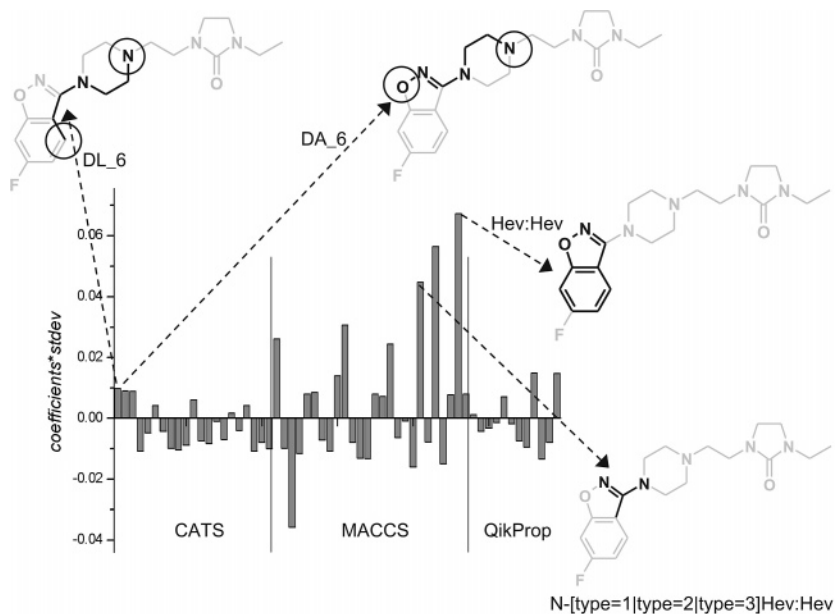


Figure 14. The PLS COEFF \times STDEV plot highlights the CATS, MACCS, and QikProp descriptors, which are positively or negatively correlated with alpha1A activity. Representative CATS and MACCS descriptors that contribute to the high-affinity binding of the depicted alpha1A antagonist are mapped onto the molecule. Also, the name of the descriptor is provided. The MACCS keys are given in Sybyl line notation (SLN).

tion” of a GPCR homology model and how the performance would be compared to those using X-ray structures

and “proper” homology models based on many template structures. Referring to the results obtained by McGov-

ern and Shoichet, we generally expect better enrichments from docking into crystal structures of proteins. On the other hand, we have previously shown that the alpha1A homology model used here as a docking template was reliable enough to identify 37 novel (out of 80 experimentally tested compounds) antagonists that show a K_i value better than 10 μM at this receptor.³⁹ These results show that in spite of the aforementioned limitations, the docking approach into a GPCR model may be well-suited for the discovery of novel GPCR antagonists.

The performance of the ligand-based Feature Tree, Catalyst 3D-pharmacophore, and PLS-DA models in identifying known antagonists is remarkable. When performing a virtual screening of a large compound library, usually only the very top-ranked compounds will be submitted for experimental testing in a biochemical assay. When only the top 1% of the ranked hit lists is considered, the presented ligand-based virtual screening strategies (except for the 3D-similarity search) achieved excellent hit rates of active compounds. Furthermore, experience from internal projects (data not shown) indicates that ligand-based virtual screening procedures frequently outperform virtual screening based on docking if sufficient ligand information for the generation of relevant models is available. Indeed, the performance of ligand-based virtual screening procedures depends critically on the amount and quality of ligand information, which is used for the generation of these models. This is particularly true for the generation of the presented PLS-DA models. We assume that the good performance of these models is due to the fact that the active compounds of the screening sets are well-represented by chemical neighbors in the training data sets, which were used for the generation of the QSAR models. Accordingly, the good performance of the Feature Tree and Catalyst pharmacophore models must be attributed to the fact that a wide range of structurally diverse active compounds for each target is available. This enabled us to select representative compounds for the generation of relevant "cross-chemotype" models. Because of the identification of relevant functional chemical groups and their abstraction into generic pharmacophores, screening methods based on such models are generally well-suited for "scaffold-hopping". Generally, we expect that the hit rates of ligand-based virtual screening approaches will be less significant if only a small amount of ligand information is available. This expectation is confirmed by the weak performance of the 3D-similarity searches, which were only based on one reference structure.

When the qualitative aspects of the generated models are considered, that is, when the possibility for interpretation is considered, the homology models are most illustrative to understand how ligands of different chemotypes potentially bind to the receptors. Validated by mutational and ligand structure-activity relationship (SAR) data, the modeled complexes provided a conclusive view on the molecular recognition process in the antagonist binding pockets. Whereas ligand-based models can only reveal binding features, which are already captured by ligands, the inclusion of complementary information from the receptor site allows for a comprehensive understanding of the molecular rec-

ognition process. Furthermore, molecular docking might be able to uncover ligands with a novel scaffold revealing a "new" binding mode, for example, by addressing additional interaction sites in the protein that have not yet been used by known ligands. In addition, protein models can be used as a structural basis for the generation of relevant binding poses and ligand alignments, which would be useful for the subsequent generation of 3D-QSAR models. Indeed, we were able to generate significant 3D-QSAR models from the docking modes of different chemical series of antagonists of the biogenic amine receptors presented in this study. Such models allow for a reliable affinity prediction within these chemical series. The structural superimposition of the receptors and the corresponding alignment of the ligands used for the generation of 3D-QSAR models thus allows for a straightforward parallel optimization of affinity and/or selectivity.

Virtual screening based on GPCR homology models may be particularly important in cases when either limited or no ligand information is available. This is true for most of the pharmaceutically relevant GPCRs, for which only the endogenous ligand is known. Once the generation of reliable GPCR structure models of the activated receptor state becomes possible,⁷⁷ molecular docking might even provide an opportunity for the identification of novel agonists. Thus, homology modeling and ligand docking might even be helpful for the deorphanization of GPCRs. As a concluding remark, we would like to point out that there is not one optimal virtual screening strategy for GPCRs. In our experience, the chance of being successful in virtual screening increases if different virtual screening approaches are employed in parallel or in combination with each other.

Experimental Section

Data Sets. Screening Set. For evaluating the performance of different virtual screening protocols, we compiled databases of active and inactive compounds from the MDDR database (MDL Information Systems Inc.). MDDR is an annotated database covering patent literature, journals, meetings, and congresses, which contains over 141 000 biologically relevant compounds and well-defined derivatives, such as drugs launched or those in the developmental phase. For the generation of the active sets, we first extracted all compounds registered as active for the considered targets, which resulted in 525 alpha1A antagonists, 656 5HT2A antagonists, 489 D2 antagonists, and 140 M1 antagonists. To ensure maximal diversity within each data set (and to avoid the inclusion of compounds coming from the same chemical series as much as possible), we extracted 50 of the most diverse compounds from each set using UNITY fingerprints (Tripos Inc., 1699 South Hanley Rd, St. Louis, MO, 63144.). Conversion of these molecules into frameworks, that is, 2D molecular structures without regard to atom type, hybridization, and bond order,⁷⁸ resulted in 48 different frameworks for the alpha1A, 47 different frameworks for the 5HT2A and D2 receptors, and 42 different frameworks for the M1 receptor, confirming the structural diversity within the active sets.

For the compilation of the inactive data set, we first randomly extracted 10 000 compounds from the MDDR and removed compounds listed as ligands of biogenic amine-binding GPCRs. From the remaining list of compounds, a diverse subset (based on UNITY fingerprints) of 1100 compounds was extracted. To avoid including compounds with biogenic amine receptor side-affinity in the inactive set, we removed 150 compounds showing structural motifs that are known to be linked to biogenic amine binding, thus, providing a database of 950 inactive compounds. Of course, this proce-

ture does not fully guarantee no side-affinity against any of the receptors considered in this study. Nevertheless, because all virtual screening strategies are evaluated against the same inactive set, we believe it is sufficiently suited for a comparative evaluation of the different screening methodologies.

Training Sets for the Generation of Catalyst Pharmacophore and Feature Tree Models. The molecules selected for the generation of Catalyst pharmacophore and Feature Tree models were extracted from the Aureus database (www.aureus-pharma.com) as described in ref 71. Aureus is a structure–activity database for GPCR ligands maintained by Aureus Pharma, which provides chemical structural information and detailed experimental conditions (e.g., assay type, cell line, or radioligand used). For each of the four GPCR targets, we only considered biological data from radioligand displacement assays, taking only high-affinity ligands into account. The challenge in the generation of models is the requirement that these models need to capture the essential interaction points for several sets of compound classes, not just for a single series. On the other hand, they should comprise sufficient interaction points to describe the important molecular characteristics that are specific for the respective receptor. Structural analysis of the selected compounds revealed that the ligand sets can be grouped into two classes for each of the four targets. Accordingly, for each target, two diverse training sets covering chemotype examples of each class (termed class1 and class2) were selected (see Figures 2–5). These ligands do not overlap with the ligands of the screening set.

Training Sets for 2D-PLS Models. (1) Active sets for the PLS models: for the generation of the PLS projection onto latent structures models, all ligands with reported K_i values (determined in a radioligand replacement assay) against the wildtype of the target receptors were extracted from the Aureus database. The resulting data sets comprised the following: 517 antagonists of the alpha1A receptor, with pK_i values ranging from 4.0 to 10.4; 509 antagonists of the 5HT2A receptor, with pK_i values ranging from 4.0 to 10.2; 420 antagonists of the D2 receptor, with pK_i values ranging from 3.8 to 9.2; and 544 M1 antagonists, with pK_i values ranging from 3.3 to 10.8.

(2) Active sets and decoy set for the PLS-DA models: a PLS-DA model was generated to predict the class membership (active or inactive at the actual target protein) of a compound. For each target receptor, we extracted all compounds with a pK_i value higher than 6, which resulted in 468 active compounds for the alpha1A receptor, 378 active compounds for the 5HT2A receptor, 287 active compounds for the D2 receptor, and 410 active compounds for the M1 receptor. Because we were interested in differentiating between active and inactive compounds (at the respective target receptors), the compilation of an additional data set of inactive compounds was necessary. This data set should provide a representative picture of inactive compounds covering a diverse chemical space of a typical screening collection. For this purpose, we compiled a “decoy data set” consisting of structurally diverse compounds from the MDDR that do not reveal affinity at the target receptors. Using a procedure similar to that used for the compilation of the screening sets, we randomly extracted 10 000 compounds, which (1) were not part of the above-described inactive data set and (2) were not explicitly stated as ligands of any other biogenic amine-binding GPCR. Again, a diverse subset (based on UNITY fingerprints) of 1100 compounds was extracted. After the compounds were removed, a process that might reveal side-affinity at the investigated receptors after visual inspection, 1000 were selected as the “decoy set” [internal evaluation studies (data not shown) indicated that larger decoy sets do not improve the prediction of the class membership of external test sets].

Quantitative Description of Hit Lists. The effectiveness of the screening methods was evaluated by assessing the hit rate and the enrichment of known active compounds within the top-scored compounds compared to that of those randomly selected.

The hit rate is given by the following equation:

$$\text{HitRate} = \left(\frac{\text{Hits}_{\text{sampled}}}{N_{\text{sampled}}} \right) 100$$

The enrichments are reported in graphical and tabular form. The enrichment factor is represented by

$$\text{EF} = \frac{\text{Hits}_{\text{sampled}}/N_{\text{sampled}}}{\text{Hits}_{\text{total}}/N_{\text{total}}}$$

in which EF is the enrichment factor, $\text{Hits}_{\text{sampled}}$ is the number of true hits in the hit list, N_{sampled} is the number of compounds in the hit list, $\text{Hits}_{\text{total}}$ is the number of hits in the full database, and N_{total} is the number of compounds in the full database.

The hit rate and enrichment factor was calculated on the basis of the assumption that all compounds with MDDR-stated activity are active (true active compounds), and compounds with no stated activity against this target are inactive. Although compounds with potential affinity against the investigated receptors were eliminated from the inactive sets after visual inspection, it cannot be excluded that some of the inactive compounds identified among the top-scored compounds by virtual screening revealed actual activity on that target. The hit rate and enrichment factor would thus be higher.

Homology Models/Docking and Scoring. Homology Modeling. A detailed description of homology model generation and validation for the alpha1A receptor is given in ref 39. We applied a modified version of the MOBILE approach (modelling binding sites including ligand information explicitly), which models proteins by homology while explicitly including information about bound ligands as restraints and thus provides more relevant geometries of protein binding sites.⁷⁹ We furthermore considered the mutational and ligand-binding data reported in the literature^{69,70} to obtain only models that were in agreement with these experimental data. Because the sequential and (probably) structural similarity among the members of the biogenic amine-binding GPCR family is high, our alpha1A receptor homology model served as a structural template for the homology modeling of the remaining three receptors covered in this study. Again, we explicitly considered ligands binding with high affinity to the respective receptors as additional restraints in the protein modeling procedure. Figure 1 shows the resulting protein–ligand complexes generated by the ligand-supported homology modeling. They served as the structural basis for the following docking experiments.

Docking and Scoring. Docking was performed using GOLD^{44–46} version 2.1 (applying “screening settings”) and FlexX-Pharm^{47,48} version 1.12.2. For each ligand, 10 poses were saved. It was our experience and that of others^{47,80,81} that better hit rates were obtained when knowledge about ligand binding was included as a restraint in the docking procedure. As mentioned before, an interaction known to be essential for biogenic amine-binding GPCRs is the (charge-mediated) hydrogen bond between Asp3.32 and a hydrogen linked to a positively ionizable nitrogen. In GOLD, this interaction was restrained by imposing a “protein H-bond” constraint (with a weighting factor of 10) for the respective carboxy oxygen of Asp3.32. Furthermore, the ligands that served as constraints for the protein modeling procedure were used as “template similarity constraints” for the virtual screening in their orientations, as depicted in Figure 1 (also applying a weighting factor of 10). A hydrogen bond with the carboxy oxygen of Asp3.32 was also constrained as being essential for docking with FlexX-Pharm. Furthermore, the positions of the positively ionizable nitrogens were extracted from the ligands depicted in Figure 1 and defined as spatial constraints in FlexX-Pharm. Prior to docking, the ligand structures were processed using the LigPrep utility from Schrodinger (Schrodinger, L. L. C., New York).

All docking poses generated by GOLD and FlexX-Pharm were rescored using seven different scoring functions (D_Score,⁸² G_Score,⁴⁴ ChemScore,⁸³ PMF,⁸⁴ and F_Score,⁴⁸ as implemented in the Cscore module of Sybyl7.0, DrugScore,⁸⁵ and Xscore⁴³). Furthermore, the scoring functions implemented as objective functions in the docking algorithms (GoldScore for GOLD, FlexX-Score for FlexX) were considered.

3D-Pharmacophore and Feature Tree Models. Feature Tree Models. The Feature Tree represents a molecular graph that is generated by the decomposition of an underlying molecule into fragments⁶ (see also Figure 6a,b). Each fragment represents a feature node, labeled with physicochemical properties. Several molecules can be combined into a consistent topological molecular alignment, resulting in an MTree model, which can be used for the virtual screening of large compound collections.⁴⁹ Such a model is conceptually similar to a 2D pharmacophore and highlights those chemical substructures that exhibit consistent protein–ligand interactions and that might be important for molecular recognition at the target protein. For easy interpretation, a graphical representation based on hexagonal grids is provided in which each node is related to topological fragments and functional groups in the input series of molecules (see Figure 6a). The matching of a candidate molecule (which is itself represented as Feature Tree) can be visualized by indicating the agreement of corresponding functional groups (Figure 6d). A similarity measure quantifies the matching of a candidate molecule with the MTree model. Database searches based on such models have been demonstrated to be efficient in virtual screening. These models are able to discover alternative molecular scaffolds not included in any of the molecules used for model generation.⁴⁹

For all molecules of the training and the screening sets, Feature Tree descriptors were calculated. For each target, the ligand sets for model generation (see Figures 2–5) were automatically converted into MTree models using the dynamic match search algorithm implemented into the Feature Tree program. In the virtual screening, all candidate ligands of the active and inactive sets were ranked according to their similarity to the MTree model used for the screening.

3D-Pharmacophore Models. A 3D-pharmacophore model (in Catalyst called a hypothesis) consists of a collection of features potentially important for the biological activity of the ligands arranged in a 3D space, such as hydrogen-bond acceptors, hydrogen-bond donors, and the hydrophobic features of a Catalyst pharmacophore model. Features are associated with position constraints that consist of the ideal location of a particular feature in a 3D space surrounded by a spherical tolerance.

The common-feature hypothesis generation (HipHop) module of Catalyst has been used for the generation of the 3D pharmacophores for the α 1A, 5HT_{2A}, D₂, and M₁ receptors.⁷¹ As mentioned above, for each target, two pharmacophore models (class1 and class2) have been generated based on the ligands depicted in Figures 2–5. For each dataset, one molecule (a representative of the class with good affinity and with a small number of conformers) was chosen as the “principal” molecule, as indicated in Figures 2–5. The following features included in the Catalyst’s features dictionary were considered for the generation of the common-feature hypothesis: positively ionizable (PI), hydrophobic (HY), hydrophobic aromatic (HYA), ring aromatic (RA), hydrogen-bond donor (HBD), and hydrogen-bond acceptor (HBA). To improve the quality of the 3D pharmacophores, a shape query was generated for each principal molecule and merged with the respective 3D pharmacophore.

For all ligands of the screening set, conformational sets were generated using the poling algorithm and the “best-quality conformational analysis” method, based on the CHARMM force field (Catalyst catConf module). In the virtual screening, the agreement of a candidate ligand with a pharmacophore was evaluated by mapping corresponding pharmacophoric features of the ligand onto the pharmacophore and calculating a fit value, which was subsequently used for the ranking of the screened library (Catalyst citest module).

2D-QSAR Models. PLS Models. For each receptor target, the molecular descriptors for all of the compounds of the training sets for the 2D-PLS models were combined with the corresponding pK_i values and used as input to create models using PLS as implemented in Sybyl7.0. To check the statistical significance of the PLS models, cross-validation runs were performed via the “leave-one-out” (LOO) procedure. Using the PLS models, we subsequently performed a virtual screening of the screening set by predicting the pK_i values of all of the candidate ligands of the active and inactive sets. Finally, the compounds were ranked according to their predicted pK_i values.

PLS-DA Models. Whereas the PLS models are trained with active compounds spanning a sufficiently large range of pK_i values, binary models are generated to predict the class membership of an external set of objects. As described above, all ligands extracted from the Aureus database exhibiting a pK_i value > 6 were considered to be active at the respective target receptors, whereas the compounds from the decoy set represented inactive compounds. A class membership variable (Y) was assigned to each active (Y = 1) and inactive (Y = 0) compound. Again, the PLS implementation in Sybyl7.0 was used for the generation and cross-validation of the models. For virtual screening, we predicted the class membership variable for all of the candidate ligands of the active and inactive sets and ranked the compounds according to the predicted values.

References

- (1) Bleicher, K. H.; Bohm, H. J.; Muller, K.; Alanine, A. I. Hit and lead generation: beyond high-throughput screening. *Nat. Rev. Drug Discovery* **2003**, *2*, 369–378.
- (2) Oprea, T. I.; Matter, H. Integrating virtual screening in lead discovery. *Curr. Opin. Chem. Biol.* **2004**, *8*, 349–358.
- (3) Sadowski, J.; Kubinyi, H. A scoring scheme for discriminating between drugs and nondrugs. *J. Med. Chem.* **1998**, *41*, 3325–3329.
- (4) Roy, K. Topological descriptors in drug design and modeling studies. *Mol. Diversity* **2004**, *8*, 321–323.
- (5) Lengauer, T.; Lemmen, C.; Rarey, M.; Zimmermann, M. Novel technologies for virtual screening. *Drug Discovery Today* **2004**, *9*, 27–34.
- (6) Rarey, M.; Dixon, J. S. Feature trees: a new molecular similarity measure based on tree matching. *J. Comput.-Aided Mol. Des.* **1998**, *12*, 471–490.
- (7) Roche, O.; Trube, G.; Zuegge, J.; Pflimlin, P.; Alanine, A.; Schneider, G. A virtual screening method for prediction of the HERG potassium channel liability of compound libraries. *Chem-BioChem* **2002**, *3*, 455–459.
- (8) Roche, O.; Schneider, P.; Zuegge, J.; Guba, W.; Kansy, M.; Alanine, A.; Bleicher, K.; Danel, F.; Gutknecht, E. M.; Rogers-Evans, M.; Neidhart, W.; Stalder, H.; Dillon, M.; Sjogren, E.; Fotouhi, N.; Gillespie, P.; Goodnow, R.; Harris, W.; Jones, P.; Taniguchi, M.; Tsujii, S.; von der Saal, W.; Zimmermann, G.; Schneider, G. Development of a virtual screening method for identification of “frequent hitters” in compound libraries. *J. Med. Chem.* **2002**, *45*, 137–142.
- (9) Lemmen, C.; Lengauer, T.; Klebe, G. FLEXS: a method for fast flexible ligand superposition. *J. Med. Chem.* **1998**, *41*, 4502–4520.
- (10) Guner, O.; Clement, O.; Kurogi, Y. Pharmacophore modeling and three-dimensional database searching for drug design using catalyst: recent advances. *Curr. Med. Chem.* **2004**, *11*, 2991–3005.
- (11) Halperin, I.; Ma, B.; Wolfson, H.; Nussinov, R. Principles of docking: an overview of search algorithms and a guide to scoring functions. *Proteins* **2002**, *47*, 409–443.
- (12) Kitchen, D. B.; Decornez, H.; Furr, J. R.; Bajorath, J. Docking and scoring in virtual screening for drug discovery: methods and applications. *Nat. Rev. Drug Discovery* **2004**, *3*, 935–949.
- (13) Sotriffer, C.; Klebe, G. Identification and mapping of small-molecule binding sites in proteins: computational tools for structure-based drug design. *Pharmacology* **2002**, *57*, 243–251.
- (14) Alvarez, J. C. High-throughput docking as a source of novel drug leads. *Curr. Opin. Chem. Biol.* **2004**, *8*, 365–370.
- (15) Brenk, R.; Naerum, L.; Gradler, U.; Gerber, H. D.; Garcia, G. A.; Reuter, K.; Stubbs, M. T.; Klebe, G. Virtual screening for submicromolar leads of tRNA-guanine transglycosylase based on a new unexpected binding mode detected by crystal structure analysis. *J. Med. Chem.* **2003**, *46*, 1133–1143.
- (16) Gruneberg, S.; Stubbs, M. T.; Klebe, G. Successful virtual screening for novel inhibitors of human carbonic anhydrase: strategy and experimental confirmation. *J. Med. Chem.* **2002**, *45*, 3588–3602.

- (17) Kraemer, O.; Hazemann, I.; Podjarny, A. D.; Klebe, G. Virtual screening for inhibitors of human aldose reductase. *Proteins* **2004**, *55*, 814–823.
- (18) Powers, R. A.; Morandi, F.; Shoichet, B. K. Structure-based discovery of a novel, noncovalent inhibitor of AmpC beta-lactamase. *Structure (Cambridge, MA, U. S.)* **2002**, *10*, 1013–1023.
- (19) Soelaiman, S.; Wei, B. Q.; Bergson, P.; Lee, Y. S.; Shen, Y.; Mrksich, M.; Shoichet, B. K.; Tang, W. J. Structure-based inhibitor discovery against adenyl cyclase toxins from pathogenic bacteria that cause anthrax and whooping cough. *J. Biol. Chem.* **2003**, *278*, 25990–25997.
- (20) Liu, H.; Li, Y.; Song, M.; Tan, X.; Cheng, F.; Zheng, S.; Shen, J.; Luo, X.; Ji, R.; Yue, J.; Hu, G.; Jiang, H.; Chen, K. Structure-based discovery of potassium channel blockers from natural products: virtual screening and electrophysiological assay testing. *Chem. Biol.* **2003**, *10*, 1103–1113.
- (21) Vangrevelinghe, E.; Zimmermann, K.; Schoepfer, J.; Portmann, R.; Fabbro, D.; Furet, P. Discovery of a potent and selective protein kinase CK2 inhibitor by high-throughput docking. *J. Med. Chem.* **2003**, *46*, 2656–2662.
- (22) Klabunde, T.; Hessler, G. Drug design strategies for targeting G-protein-coupled receptors. *ChemBioChem* **2002**, *3*, 928–944.
- (23) Flohr, S.; Kurz, M.; Kostenis, E.; Brkovich, A.; Fournier, A.; Klabunde, T. Identification of nonpeptidic urotensin II receptor antagonists by virtual screening based on a pharmacophore model derived from structure–activity relationships and nuclear magnetic resonance studies on urotensin II. *J. Med. Chem.* **2002**, *45*, 1799–1805.
- (24) Marriott, D. P.; Dougall, I. G.; Meghani, P.; Liu, Y. J.; Flower, D. R. Lead generation using pharmacophore mapping and three-dimensional database searching: application to muscarinic M(3) receptor antagonists. *J. Med. Chem.* **1999**, *42*, 3210–3216.
- (25) Kalani, M. Y.; Vaidehi, N.; Hall, S. E.; Trabanino, R. J.; Freddolino, P. L.; Kalani, M. A.; Floriano, W. B.; Kam, V. W.; Goddard, W. A., III The predicted 3D structure of the human D2 dopamine receptor and the binding site and binding affinities for agonists and antagonists. *Proc. Natl. Acad. Sci. U.S.A.* **2004**, *101*, 3815–3820.
- (26) Freddolino, P. L.; Kalani, M. Y.; Vaidehi, N.; Floriano, W. B.; Hall, S. E.; Trabanino, R. J.; Kam, V. W.; Goddard, W. A., III Predicted 3D structure for the human beta 2 adrenergic receptor and its binding site for agonists and antagonists. *Proc. Natl. Acad. Sci. U.S.A.* **2004**, *101*, 2736–2741.
- (27) Vaidehi, N.; Floriano, W. B.; Trabanino, R.; Hall, S. E.; Freddolino, P.; Choi, E. J.; Zamanakos, G.; Goddard, W. A., III Prediction of structure and function of G protein-coupled receptors. *Proc. Natl. Acad. Sci. U.S.A.* **2002**, *99*, 12622–12627.
- (28) Evers, A.; Klebe, G. Successful virtual screening for a submicromolar antagonist of the neurokinin-1 receptor based on a ligand-supported homology model. *J. Med. Chem.* **2004**, *47*, 5381–5392.
- (29) Costanzi, S.; Mamedova, L.; Gao, Z. G.; Jacobson, K. A. Architecture of P2Y nucleotide receptors: structural comparison based on sequence analysis, mutagenesis, and homology modeling. *J. Med. Chem.* **2004**, *47*, 5393–5404.
- (30) Broer, B. M.; Gurrath, M.; Holtje, H. D. Molecular modelling studies on the ORL1-receptor and ORL1-agonists. *J. Comput.-Aided Mol. Des.* **2003**, *17*, 739–754.
- (31) Furse, K. E.; Lybrand, T. P. Three-dimensional models for beta-adrenergic receptor complexes with agonists and antagonists. *J. Med. Chem.* **2003**, *46*, 4450–4462.
- (32) Johren, K.; Holtje, H. D. A model of the human M2 muscarinic acetylcholine receptor. *J. Comput.-Aided Mol. Des.* **2002**, *16*, 795–801.
- (33) Lavecchia, A.; Greco, G.; Novellino, E.; Vittorio, F.; Ronsisvalle, G. Modeling of kappa-opioid receptor/agonists interactions using pharmacophore-based and docking simulations. *J. Med. Chem.* **2000**, *43*, 2124–2134.
- (34) Pedretti, A.; Elena, S. M.; Villa, L.; Vistoli, G. Binding site analysis of full-length alpha1A adrenergic receptor using homology modeling and molecular docking. *Biochem. Biophys. Res. Commun.* **2004**, *319*, 493–500.
- (35) Salo, O. M.; Lahtela-Kakkonen, M.; Gynther, J.; Jarvinen, T.; Poso, A. Development of a 3D model for the human cannabinoid CB1 receptor. *J. Med. Chem.* **2004**, *47*, 3048–3057.
- (36) Shim, J. Y.; Welsh, W. J.; Howlett, A. C. Homology model of the CB1 cannabinoid receptor: sites critical for nonclassical cannabinoid agonist interaction. *Biopolymers* **2003**, *71*, 169–189.
- (37) Hardin, C.; Pogorelov, T. V.; Luthey-Schulten, Z. Ab initio protein structure prediction. *Curr. Opin. Struct. Biol.* **2002**, *12*, 176–181.
- (38) Bissantz, C.; Bernard, P.; Hibert, M.; Rognan, D. Protein-based virtual screening of chemical databases. II. Are homology models of G-protein coupled receptors suitable targets? *Proteins* **2003**, *50*, 5–25.
- (39) Evers, A.; Klabunde, T. Structure-based drug discovery using GPCR homology modeling: successful virtual screening for antagonists of the alpha1A adrenergic receptor. *J. Med. Chem.* **2005**, *48*, 1088–1097.
- (40) Varady, J.; Wu, X.; Fang, X.; Min, J.; Hu, Z.; Levant, B.; Wang, S. Molecular modeling of the three-dimensional structure of dopamine 3 (D3) subtype receptor: discovery of novel and potent D3 ligands through a hybrid pharmacophore- and structure-based database searching approach. *J. Med. Chem.* **2003**, *46*, 4377–4392.
- (41) Dixon, J. S. Evaluation of the CASP2 docking section. *Proteins* **1997**, Suppl. 1, 198–204.
- (42) Ferrara, P.; Gohlke, H.; Price, D. J.; Klebe, G.; Brooks, C. L., III Assessing scoring functions for protein–ligand interactions. *J. Med. Chem.* **2004**, *47*, 3032–3047.
- (43) Wang, R.; Lu, Y.; Wang, S. Comparative evaluation of 11 scoring functions for molecular docking. *J. Med. Chem.* **2003**, *46*, 2287–2303.
- (44) Jones, G.; Willett, P.; Glen, R. C.; Leach, A. R.; Taylor, R. Development and validation of a genetic algorithm for flexible docking. *J. Mol. Biol.* **1997**, *267*, 727–748.
- (45) Jones, G.; Willett, P.; Glen, R. C. Molecular recognition of receptor sites using a genetic algorithm with a description of desolvation. *J. Mol. Biol.* **1995**, *245*, 43–53.
- (46) Verdonk, M. L.; Cole, J. C.; Hartshorn, M. J.; Murray, C. W.; Taylor, R. D. Improved protein–ligand docking using GOLD. *Proteins* **2003**, *52*, 609–623.
- (47) Hindle, S. A.; Rarey, M.; Buning, C.; Lengauer, T. Flexible docking under pharmacophore type constraints. *J. Comput.-Aided Mol. Des.* **2002**, *16*, 129–149.
- (48) Rarey, M.; Kramer, B.; Lengauer, T.; Klebe, G. A fast flexible docking method using an incremental construction algorithm. *J. Mol. Biol.* **1996**, *261*, 470–489.
- (49) Hessler, G.; Zimmermann, M.; Matter, H.; Evers, A.; Naumann, T.; Lengauer, T.; Rarey, M. Multiple-ligand-based virtual screening: Methods and Applications of the m-tree approach. *J. Med. Chem.*, in press.
- (50) Schneider, G.; Clement-Chomienne, O.; Hilfiger, L.; Schneider, P.; Kirsch, S.; Bohm, H. J.; Neidhart, W. Virtual screening for bioactive molecules by evolutionary de novo design special thanks to Neil R. Taylor for his help in preparation of the manuscript. *Angew. Chem., Int. Ed.* **2000**, *39*, 4130–4133.
- (51) Schneider, G.; Neidhart, W.; Giller, T.; Schmid, G. “Scaffold-hopping” by topological pharmacophore search: a contribution to virtual screening. *Angew. Chem., Int. Ed.* **1999**, *38*, 2894–2896.
- (52) Grethe, G.; Moock, T. E. Similarity searching in REACCS. A new tool for the synthetic chemist. *J. Chem. Inf. Comput. Sci.* **1990**, *30*, 511–520.
- (53) Jorgensen, W. L.; Duffy, E. M. Prediction of drug solubility from structure. *Adv. Drug Delivery Rev.* **2002**, *54*, 355–366.
- (54) Jorgensen, W. L.; Duffy, E. M. Prediction of drug solubility from Monte Carlo simulations. *Bioorg. Med. Chem. Lett.* **2000**, *10*, 1155–1158.
- (55) Pirard, B.; Pickett, S. D. Classification of kinase inhibitors using BCUT descriptors. *J. Chem. Inf. Comput. Sci.* **2000**, *40*, 1431–1440.
- (56) Matter, H. Selecting optimally diverse compounds from structure databases: a validation study of two-dimensional and three-dimensional molecular descriptors. *J. Med. Chem.* **1997**, *40*, 1219–1229.
- (57) Matter, H. Computational approaches towards the quantification of molecular diversity and design of compound libraries. *EXS* **2003**, 125–156.
- (58) Cramer, R. D.; Poss, M. A.; Hermsmeier, M. A.; Caulfield, T. J.; Kowala, M. C.; Valentine, M. T. Prospective identification of biologically active structures by toponer shape similarity searching. *J. Med. Chem.* **1999**, *42*, 3919–3933.
- (59) Hert, J.; Willett, P.; Wilton, D. J.; Acklin, P.; Azzaoui, K.; Jacoby, E.; Schuffenhauer, A. Comparison of topological descriptors for similarity-based virtual screening using multiple bioactive reference structures. *Org. Biomol. Chem.* **2004**, *2*, 3256–3266.
- (60) Hert, J.; Willett, P.; Wilton, D. J.; Acklin, P.; Azzaoui, K.; Jacoby, E.; Schuffenhauer, A. Comparison of fingerprint-based methods for virtual screening using multiple bioactive reference structures. *J. Chem. Inf. Comput. Sci.* **2004**, *44*, 1177–1185.
- (61) Schuffenhauer, A.; Gillet, V. J.; Willett, P. Similarity searching in files of three-dimensional chemical structures: analysis of the BIOSTER database using two-dimensional fingerprints and molecular field descriptors. *J. Chem. Inf. Comput. Sci.* **2000**, *40*, 295–307.
- (62) Mason, J. S.; Morize, I.; Menard, P. R.; Cheney, D. L.; Hulme, C.; Labaudiniere, R. F. New 4-point pharmacophore method for molecular similarity and diversity applications: overview of the method and applications, including a novel approach to the design of combinatorial libraries containing privileged substructures. *J. Med. Chem.* **1999**, *42*, 3251–3264.

- (63) Sun, H. Prediction of chemical carcinogenicity from molecular structure. *J. Chem. Inf. Comput. Sci.* **2004**, *44*, 1506–1514.
- (64) Shen, M.; Beguin, C.; Golbraikh, A.; Stables, J. P.; Kohn, H.; Tropsha, A. Application of predictive QSAR models to database mining: identification and experimental validation of novel anticonvulsant compounds. *J. Med. Chem.* **2004**, *47*, 2356–2364.
- (65) Baurin, N.; Mozziconacci, J. C.; Arnoult, E.; Chavatte, P.; Marot, C.; Morin-Allory, L. 2D QSAR consensus prediction for high-throughput virtual screening. An application to COX-2 inhibition modeling and screening of the NCI database. *J. Chem. Inf. Comput. Sci.* **2004**, *44*, 276–285.
- (66) Sutherland, J. J.; O'Brien, L. A.; Weaver, D. F. A comparison of methods for modeling quantitative structure–activity relationships. *J. Med. Chem.* **2004**, *47*, 5541–5554.
- (67) Roche, O.; Trube, G.; Zuegge, J.; Pflimlin, P.; Alanine, A.; Schneider, G. A virtual screening method for prediction of the HERG potassium channel liability of compound libraries. *ChemBioChem* **2002**, *3*, 455–459.
- (68) Shi, L.; Javitch, J. A. The binding site of aminergic G protein-coupled receptors: the transmembrane segments and second extracellular loop. *Annu. Rev. Pharmacol. Toxicol.* **2002**, *42*, 437–467.
- (69) Hamaguchi, N.; True, T. A.; Saussy, D. L., Jr.; Jeffs, P. W. Phenylalanine in the second membrane-spanning domain of alpha 1A-adrenergic receptor determines subtype selectivity of dihydropyridine antagonists. *Biochemistry* **1996**, *35*, 14312–14317.
- (70) Hamaguchi, N.; True, T. A.; Goetz, A. S.; Stouffer, M. J.; Lybrand, T. P.; Jeffs, P. W. Alpha 1-adrenergic receptor subtype determinants for 4-piperidyl oxazole antagonists. *Biochemistry* **1998**, *37*, 5730–5737.
- (71) Klabunde, T.; Evers, A. GPCR anti-target modeling: pharmacophore models for biogenic amine binding GPCRs to avoid GPCR-mediated side-effects. *ChemBioChem* **2005**, *6*, 876–889.
- (72) Sheridan, R. P.; Feuston, B. P.; Maiorov, V. N.; Kearsley, S. K. Similarity to molecules in the training set is a good discriminator for prediction accuracy in QSAR. *J. Chem. Inf. Comput. Sci.* **2004**, *44*, 1912–1928.
- (73) Schnecke, V.; Swanson, C. A.; Getzoff, E. D.; Tainer, J. A.; Kuhn, L. A. Screening a peptidyl database for potential ligands to proteins with side-chain flexibility. *Proteins* **1998**, *33*, 74–87.
- (74) Schnecke, V.; Kuhn, L. A. Database screening for HIV protease ligands: the influence of binding-site conformation and representation on ligand selectivity. *Proc. Int. Conf. Intell. Syst. Mol. Biol.* **1999**, 242–251.
- (75) Ewing, T. J.; Makino, S.; Skillman, A. G.; Kuntz, I. D. DOCK 4.0: search strategies for automated molecular docking of flexible molecule databases. *J. Comput.-Aided Mol. Des.* **2001**, *15*, 411–428.
- (76) McGovern, S. L.; Shoichet, B. K. Information decay in molecular docking screens against holo, apo, and modeled conformations of enzymes. *J. Med. Chem.* **2003**, *46*, 2895–2907.
- (77) Gouldson, P. R.; Kidley, N. J.; Bywater, R. P.; Psaroudakis, G.; Brooks, H. D.; Diaz, C.; Shire, D.; Reynolds, C. A. Toward the active conformations of rhodopsin and the beta2-adrenergic receptor. *Proteins* **2004**, *56*, 67–84.
- (78) Bemis, G. W.; Murcko, M. A. The properties of known drugs. 1. Molecular frameworks. *J. Med. Chem.* **1996**, *39*, 2887–2893.
- (79) Evers, A.; Gohlke, H.; Klebe, G. Ligand-supported homology modelling of protein binding-sites using knowledge-based potentials. *J. Mol. Biol.* **2003**, *334*, 327–345.
- (80) Good, A. C.; Cheney, D. L.; Sitkoff, D. F.; Tokarski, J. S.; Stouch, T. R.; Bassolino, D. A.; Krystek, S. R.; Li, Y.; Mason, J. S.; Perkins, T. D. Analysis and optimization of structure-based virtual screening protocols. 2. Examination of docked ligand orientation sampling methodology: mapping a pharmacophore for success. *J. Mol. Graphics Modell.* **2003**, *22*, 31–40.
- (81) Fradera, X.; Knegtel, R. M.; Mestres, J. Similarity-driven flexible ligand docking. *Proteins* **2000**, *40*, 623–636.
- (82) Kuntz, I. D.; Blaney, J. M.; Oatley, S. J.; Langridge, R.; Ferrin, T. E. A geometric approach to macromolecule–ligand interactions. *J. Mol. Biol.* **1982**, *161*, 269–288.
- (83) Eldridge, M. D.; Murray, C. W.; Auton, T. R.; Paolini, G. V.; Mee, R. P. Empirical scoring functions: I. The development of a fast empirical scoring function to estimate the binding affinity of ligands in receptor complexes. *J. Comput.-Aided Mol. Des.* **1997**, *11*, 425–445.
- (84) Muegge, I.; Martin, Y. C. A general and fast scoring function for protein–ligand interactions: a simplified potential approach. *J. Med. Chem.* **1999**, *42*, 791–804.
- (85) Gohlke, H.; Hendlich, M.; Klebe, G. Knowledge-based scoring function to predict protein–ligand interactions. *J. Mol. Biol.* **2000**, *295*, 337–356.
- (86) Kehne, J. H.; Baron, B. M.; Carr, A. A.; Chaney, S. F.; Elands, J.; Feldman, D. J.; Frank, R. A.; van Giersbergen, P. L.; McCloskey, T. C.; Johnson, M. P.; McCarty, D. R.; Poirrot, M.; Senyah, Y.; Siegel, B. W.; Widmaier, C. Preclinical characterization of the potential of the putative atypical antipsychotic MDL 100,907 as a potent 5-HT_{2A} antagonist with a favorable CNS safety profile. *J. Pharmacol. Exp. Ther.* **1996**, *277*, 968–981.
- (87) Corbett, R.; Hartman, H.; Kerman, L. L.; Woods, A. T.; Strupczewski, J. T.; Helsley, G. C.; Conway, P. C.; Dunn, R. W. Effects of atypical antipsychotic agents on social behavior in rodents. *Pharmacol., Biochem. Behav.* **1993**, *45*, 9–17.
- (88) Mitsuya, M.; Kobayashi, K.; Kawakami, K.; Satoh, A.; Ogino, Y.; Kakikawa, T.; Ohtake, N.; Kimura, T.; Hirose, H.; Sato, A.; Numazawa, T.; Hasegawa, T.; Noguchi, K.; Mase, T. A potent, long-acting, orally active (2*R*)-2-[(1*R*)-3,3-difluorocyclopentyl]-2-hydroxy-2-phenylacetamide: novel muscarinic M(3) receptor antagonist with high selectivity for M(3) over M(2) receptors. *J. Med. Chem.* **2000**, *43*, 5017–5029.

JM0500900